PNAS
www.pnas.org

Supplementary Information for

Design-functionality relationships for adhesion/growth-regulatory galectins

Anna-Kristin Ludwig, Malwina Michalak, Qi Xiao, Ulrich Gilles, Francisco J. Medrano, Hanyue Ma, Forrest G. FitzGerald, William D. Hasley, Adriel Melendez-Davila, Matthew Liu, Khosrow Rahimi, Nina Yu. Kostina, Cesar Rodriguez-Emmenegger, Martin Möller, Ingo Lindner, Herbert Kaltner, Mare Cudic, Dietmar Reusch, Jürgen Kopitz, Antonio Romero, Stefan Oscarson, Michael L. Klein, Hans-Joachim Gabius, Virgil Percec,

Michael L. Klein
Email: mlklein@temple.edu
Hans-Joachim Gabius
Email: gabius@tiph.vetmed.uni-muenchen.de
Virgil Percec
Email: percec@sas.upenn.edu

This PDF file includes:

Supplementary text
Figs. S1 to S26
Tables S1 to S6
References for SI reference citations

Other supplementary materials for this manuscript include the following:

Dataset S1

www.pnas.org/cgi/doi/10.1073/pnas.1813515116

Supplementary Information Text

1. cDNA engineering and protein production

As template DNA for the generation of cDNAs for the set of Gal-3 and Gal-1 homo- and heterodimers as well as 8S-linked homo- and heterodimers plasmids coding for the wild-type proteins of Gal-1, Gal-3, Gal-8S and Gal-8L were used for the three-step PCR procedure previously described for the Gal-1-based homodimers (1). Primers for the different galectin constructs were listed in the Table below. Exemplarily, the steps to construct the Gal-3—Gal-3 and Gal-3—8S—Gal-3 plasmids were given as follows:

1) the coding sequence for the N-terminal CRD was obtained by using a forward flanking oligonucleotide containing an internal *Nde*I restriction site (5'-GCTCATATGGGCGCCCCTGCTGGGC-3') and a reverse oligonucleotide (5′-GGCCCAGCAGGGGCGCCTATCATGGTATATGAAGCACTG-3′ (Gal-3—Gal-3) or 5′-GTCCGAGCTGAAGCTAAATATCATGGTATATGAAGCAC-3′(8S)) with a sequence specific for the connected region (GG or linker 8S).
2) the linker sequence of Gal-8S was amplified using oligonucleotides with overlapping parts to the N-terminal (5′-GTGCTTCATATACCATGATATTTAGCTTCAGCTCGGAC-3′) and the C-terminal (5′- GGCCCAGCAGGGGCGCCAAGCTGGGGCGTGCCAG-3′) sequence of Gal-1.
3) the nucleotide sequence for the C-terminal CRD was amplified using a forward oligonucleotide containing a sequence complementary to the linker region connected with the CRD (5′-CAGTGCTTCATATACCATGATAGGCGCCCCTGCTGGGCC-3′ (Gal-3—Gal-3) or 5′- ctggcacgccccagcttGGCGCCCCTGCTGGGCC-3′ (8S)) and the reverse flanking primer with an internal *Hind*III restriction site (5′-cgtaagctttcagtcaaaggccacac-3′).

The obtained two (Gal-3—Gal-3) or three (8S) fragments with overlapping regions were purified and served as templates for PCR using Phusion High Fidelity Polymerase™ (New England BioLabs, Frankfurt, Germany). For this PCR setup the forward flanking oligonucleotides with *Nde*I restriction side and the reverse flanking oligonucleotides with the *Hind*III restriction side were used to generate the complete cDNA sections which then

consist of the nucleotide sequence for the N-terminal CRD associated with/without a linker sequence attached to the C-terminal CRD. The gel-purified fragments were digested by using the restriction enzymes *Nde*I and *Hind*III and then ligated into a *Nde*I/*Hind*III-cuted pGEMEX-1 vector (Promega, Mannheim, Germany) which was amplified in bacteria after transformation. The sequence was verified by DNA sequencing. The plasmid was transformed into *Escherichia coli* BL21 (DE3)-pLysS (Promega) for recombinant production. Bacteria cells were grown in LB medium (Roth, Karlsruhe, Germany) containing the appropriate antibiotics for 16 h at 37 °C and then transferred to TB (Roth) medium. After initial growth for 2 – 3 h at 37 °C up to 0.6 – 0.8 (OD_{600nm}), gene expression was induced using 100 µM or 50 µM isopropyl-β-1-thio-*D*-galactopyranoside (IPTG) for homo-/heterodimers and Gal-3NT/1, respectively. After induction bacteria were cultured at 22 °C for additional 16 h. The protein was purified from bacterial extracts by affinity chromatography on lactosylated Sepharose 4B, as previously described (2), with yields in a range from 17.86 mg/L (Gal-3—Gal-1) to 81.69 mg/L (Gal-1—Gal-3). Purity was ascertained by one-dimensional gel electrophoresis under denaturing conditions, gel filtration and mass spectrometry (MALDI-TOF, peptide fingerprinting). For SAXS analysis proteins were precipitated by addition of ammonium sulfate up to 80% saturation. Primers for amplification of nucleotide sequences and sequence information for each protein are listed below.

Galectin	Primer	Sequence
Gal-3NT/1	hGal-3_NdeI-FOR	5′GCTCATATGGCAGACAATTTTTCGCTC′3
	hGal1_Hind_REV	5′CGTAAGCTTTCAGTCAAAGGCCACAC′3
	Gal-3NT/1_FOR	5′CCTGCCACTGGCCCCTATGCTTGTGGTCTGGTCGCCAGC′3
	Gal-3NT/1_REV	5′GCTGGCGACCAGACCACAAGCATAGGGGCCAGTGGCAGG′3
Gal-3—Gal-3	hGal3_hGal3_FOR	5′CAGTGCTTCATATACCATGATAGGCGCCCCTGCTGGGCC′3
	hGal3_hGal3_REV	5′GGCCCAGCAGGGGCGCCTATCATGGTATATGAAGCACTG′3
	trGal-3_NdeI-FOR	5′GCTCATATGGGCGCCCCTGCTGGGC′3
	Gal-3_HindIII-rev	5′CGAAAGCTTTTAGATCTGGACATAGGACAAGGTG′3
Gal-3—8S—Gal-3	hGal3_8S_FOR	5′GTGCTTCATATACCATGATATTTAGCTTCAGCTCGGAC′3
	hGal3_8S_REV	5′GTCCGAGCTGAAGCTAAATATCATGGTATATGAAGCAC′3
	trGal-3_NdeI-For	5′GCTCATATGGGCGCCCCTGCTGGGC′3
	Gal-3_HindIII-REV	5′CGAAAGCTTTTAGATCTGGACATAGGACAAGGTG′3
Gal-3—8L—Gal-3	8L-Gal-3-FOR	5′GAACTATGTGTCAAAGGGCGCCCCTGCTGGGC′3
	8L-Gal-3-REV	5′GCCCAGCAGGGGCGCCCTTTGACACATAGTTC′3
	Gal-3-8L-REV	5′CGAGCTGAAGCTAAATATCATGGTATATGAAGC′3
	Gal-3-8L FOR	5′GCTTCATATACCATGATATTTAGCTTCAGCTCG′3
	trGal-3_NdeI-FOR	5′GCTCATATGGGCGCCCCTGCTGGGC′3
	Gal-3_HindIII-REV	5′CGAAAGCTTTTAGATCTGGACATAGGACAAGGTG′3

Gal-3—Gal-1	hGal3_hGal1_FOR	5′CAGTGCTTCATATACCATGATAGCTTGTGGTCTGGTCGCC′3
	hGal3_hGal1_REV	5′GGCGACCAGACCACAAGCTATCATGGTATATGAAGCACTG′3
	trGal-3_NdeI-FOR	5′GCTCATATGGGCGCCCCTGCTGGGC′3
	hGal1_Hind_REV	CGTAAGCTTTCAGTCAAAGGCCACAC′3
Gal-3—8S—Gal-1	hGal3_8S_FOR	5′GTGCTTCATATACCATGATATTTAGCTTCAGCTCGGAC′3
	hGal3_8S_REV	5′GTCCGAGCTGAAGCTAAATATCATGGTATATGAAGCAC′3
	hGal1_LS_FOR	5′CAAATGTGTGGCCTTTGACTTTAGCTTCAGCTCGGACTTAC′3
	hGal1_LS_REV	5′GCGACCAGACCACAAGCAAGCTGGGGCGTGCCAG′3
	trGal-3_NdeI-FOR	5′GCTCATATGGGCGCCCCTGCTGGGC′3
	hGal1_Hind_REV	CGTAAGCTTTCAGTCAAAGGCCACAC′3
Gal-1—Gal-3	Gal-3_HindIII-REV	5′CGAAAGCTTTTAGATCTGGACATAGGACAAGGTG′3
	hGal1_Nde_FOR	5′GCACATATGGCTTGTGGTCTGGTC′3
	hGal1_hGal3_FOR	5′CAAATGTGTGGCCTTTGACGGCGCCCCTGCTGGGCC′3
	hGal1_hGal3_REV	5′GGCCCAGCAGGGGCGCCGTCAAAGGCCACACATTTG′3
Gal-1—8S—Gal-3	hGal1_LS_2_FOR	5′CTGGCACGCCCCAGCTTGCTTGTGGTCTGGTCGC′3
	hGal1_LS_2_REV	5′GTAAGTCCGAGCTGAAGCTAAAGTCAAAGGCCACACATTTG′3
	8S_hGal3_FOR	5′CTGGCACGCCCCAGCTTGGCGCCCCTGCTGGGCC′3
	8S_hGal3_REV	5′GGCCCAGCAGGGGCGCCAAGCTGGGGCGTGCCAG′3
	hGal1_Nde_FOR	5′GCACATATGGCTTGTGGTCTGGTC′3
	Gal-3_HindIII-REV	5′CGAAAGCTTTTAGATCTGGACATAGGACAAGGTG′3

Amino acid Sequence:

Gal-3NT/1 (24739.49 Da)

MADNFSLHDALSGSGNPNPQGWPGAWGNQPAGAGGYPGASYPGAYPGQAPPG
AYPGQAPPGAYHGAPGAYPGAPAPGVYPGPPSGPGAYPSSGQPSAPGAYPATGP
YACGLVASNLNLKPGECLRVRGEVAPDAKSFVLNLGKDSNNLCLHFNPRFNAH
GDANTIVCNSKDGGAWGTEQREAVFPFQPGSVAEVCITFDQANLTVKLPDGYEF
KFPNRLNLEAINYMAADGDFKIKCVAFD

Gal-3—Gal-3 (32180.11 Da)

MGAPAGPLIVPYNLPLPGGVVPRMLITILGTVKPNANRIALDFQRGNDVAFHFNP
RFNENNRRVIVCNTKLDNNWGREERQSVFPFESGKPFKIQVLVEPDHFKVAVND
AHLLQYNHRVKKLNEISKLGISGDIDLTSASYTMIGAPAGPLIVPYNLPLPGGVVP
RMLITILGTVKPNANRIALDFQRGNDVAFHFNPRFNENNRRVIVCNTKLDNNWG
REERQSVFPFESGKPFKIQVLVEPDHFKVAVNDAHLLQYNHRVKKLNEISKLGIS
GDIDLTSASYTMI

Gal-3—8S—Gal-3 (35746.99 Da)

MGAPAGPLIVPYNLPLPGGVVPRMLITILGTVKPNANRIALDFQRGNDVAFHFNP
RFNENNRRVIVCNTKLDNNWGREERQSVFPFESGKPFKIQVLVEPDHFKVAVND
AHLLQYNHRVKKLNEISKLGISGDIDLTSASYTMIFSFSSDLQSTQASSLELTEISR
ENVPKSGTPQLGAPAGPLIVPYNLPLPGGVVPRMLITILGTVKPNANRIALDFQRG
NDVAFHFNPRFNENNRRVIVCNTKLDNNWGREERQSVFPFESGKPFKIQVLVEPD
HFKVAVNDAHLLQYNHRVKKLNEISKLGISGDIDLTSASYTMI

Gal-1—Gal-3 (30731.20 Da)

MACGLVASNLNLKPGECLRVRGEVAPDAKSFVLNLGKDSNNLCLHFNPRFNAH
GDANTIVCNSKDGGAWGTEQREAVFPFQPGSVAEVCITFDQANLTVKLPDGYEF
KFPNRLNLEAINYMAADGDFKIKCVAFDGAPAGPLIVPYNLPLPGGVVPRMLITI
LGTVKPNANRIALDFQRGNDVAFHFNPRFNENNRRVIVCNTKLDNNWGREERQS

VFPFESGKPFKIQVLVEPDHFKVAVNDAHLLQYNHRVKKLNEISKLGISGDIDLTS
ASYTMI

Gal-3—Gal-1 (30731.20 Da)
MGAPAGPLIVPYNLPLPGGVVPRMLITILGTVKPNANRIALDFQRGNDVAFHFNP
RFNENNRRVIVCNTKLDNNWGREERQSVFPFESGKPFKIQVLVEPDHFKVAVND
AHLLQYNHRVKKLNEISKLGISGDIDLTSASYTMIACGLVASNLNLKPGECLRVR
GEVAPDAKSFVLNLGKDSNNLCLHFNPRFNAHGDANTIVCNSKDGGAWGTEQR
EAVFPFQPGSVAEVCITFDQANLTVKLPDGYEFKFPNRLNLEAINYMAADGDFKI
KCVAFD

Gal-3—8S—Gal-1 (34298.08 Da)
MGAPAGPLIVPYNLPLPGGVVPRMLITILGTVKPNANRIALDFQRGNDVAFHFNP
RFNENNRRVIVCNTKLDNNWGREERQSVFPFESGKPFKIQVLVEPDHFKVAVND
AHLLQYNHRVKKLNEISKLGISGDIDLTSASYTMIFSFSSDLQSTQASSLELTEISR
ENVPKSGTPQLACGLVASNLNLKPGECLRVRGEVAPDAKSFVLNLGKDSNNLCL
HFNPRFNAHGDANTIVCNSKDGGAWGTEQREAVFPFQPGSVAEVCITFDQANLT
VKLPDGYEFKFPNRLNLEAINYMAADGDFKIKCVAFD

Gal-3—8L—Gal-3 (40091.90 Da)
MGAPAGPLIVPYNLPLPGGVVPRMLITILGTVKPNANRIALDFQRGNDVAFHFNP
RFNENNRRVIVCNTKLDNNWGREERQSVFPFESGKPFKIQVLVEPDHFKVAVND
AHLLQYNHRVKKLNEISKLGISGDIDLTSASYTMIFSFSSDLQSTQASSLELTEISR
ENVPKSGTPQLPSNRGGDISKIAPRTVYTKSKDSTVNHTLTCTKIPPMNYVSKGA
PAGPLIVPYNLPLPGGVVPRMLITILGTVKPNANRIALDFQRGNDVAFHFNPRFNE
NNRRVIVCNTKLDNNWGREERQSVFPFESGKPFKIQVLVEPDHFKVAVNDAHLL
QYNHRVKKLNEISKLGISGDIDLTSASYTMI

MS analysis

To confirm the amino acid sequence and to exclude presence of any post-translational modification all galectin variants were examined by matrix-assisted laser desorption/ionization (MALDI) time-of-flight (TOF) mass spectrometry. To this end the galectin constructs were characterized in a top-down approach by in-source decay (ISD), while peptides from protease-digested protein were analyzed in a bottom-up approach by peptide mass fingerprinting. The samples were dissolved in water to reach a final concentration of 100 pmol/µL. For ISD processing with sinapinic acid (SA) as matrix, the protein-containing sample was further diluted with 0.1% trifluoroacetic acid (TFA) to a final concentration of 20 pmol/µL. 0.5 µL of saturated solution of SA in ethanol were pipetted on individual spots of the MALDI target. After drying, 1 µL of protein solution was added on top of the thin SA layer, immediately followed by 1 µL of saturated solution of SA in 0.1% TFA with 30% acetonitrile (TA30). For fingerprinting with tryptic and

chymotryptic digestion all solutions were prepared in digestion buffers: 40 mM NH_4HCO_3 or 100 mM Tris HCl (pH 7.8), respectively. 10 µg of protein was dissolved in 10 µL of appropriate digestion buffer and treated with 2 µL of a 10 mM solution of dithiothreitol (DTT) for 1 h at 45 °C to completely reduce disulfide bonds, the thiol groups were then alkylated by addition of 1 µL of a solution of 55 mM iodoacetamide for 30 min at 25 °C and after adding 2.5 µL of 10 mM DTT, the mixture was incubated for 15 min at 37 °C to let all iodoacetamide react with a thiol group. Tryptic digestion was performed with 100 ng trypsin in 40 mM NH_4HCO_3 solution overnight at 37 °C. Sample was diluted in solution containing 50% acetonitrile in 0.1% TFA (TA50) (1:5, v/v) and 1 µL of sample was then pipetted on individual spots of the MALDI target followed by 1 µL of a saturated solution of α-cyano-4-hydroxy-cinnamic acid in TA50 (HCCA). Chymotryptic digestion was performed with 100 ng chymotrypsin in 100 mM Tris HCl (pH 7.8) for 3 h at 25 °C and was stopped by addition of 2.5 µL 0.1% TFA. Sample was desalted using zip-tip C18 (Merck Millipore, Darmstadt, Germany) according to the manufacturer's instructions. Peptides were eluted from zip-tip with 2 µL of HCCA and directly spotted on the MALDI target. Spotted samples were dried at ambient temperature prior to mass-spectrometric analysis. All matrices were obtained from Bruker Daltonik (Bremen, Germany).

MALDI mass spectra were collected on an Ultraflex™ TOFTOF I instrument (Bruker Daltonik) equipped with a nitrogen laser (20 Hz), as described for variants of human Gal-1 variants recently (3). For samples prepared with the SA matrix, reflectron in-source decay (reISD) spectra were recorded in the positive-ion reflectron mode using the following settings: ion acceleration voltage at 25.0 kV, reflector voltage at 26.3 kV, first extraction plate at 21.75 kV. Linear in-source decay (linISD) spectra were measured in the positive-ion linear mode with settings for ion acceleration voltage at 25.0 kV and first extraction plate at 23.2 kV. For molecular weight determination intact proteins were analyzed in the positive-ion linear mode using the following settings: ion acceleration voltage at 25.0 kV and first extraction plate at 23 kV. For peptide fingerprinting, the positive-ion reflectron mode with ion acceleration voltage at 25.0 kV, reflector voltage at 26.3 kV and first extraction plate at 21.75 kV were set. Experimental information from up to 5000 individual laser shots was routinely accumulated. Calibration of spectra was performed externally by a linear fit using the protein calibration standard II for proteins, by a quadratic fit using the protein standard I for linISD or the peptide calibration standard II for reISD spectra and

fingerprinting (Bruker Daltonik). FlexControl version 2.4 was used for instrument control and FlexAnalysis version 2.4 for processing the data of the spectra. Annotated spectra were further analyzed by BioTools 3.0 (Bruker Daltonik).

Gel filtration

Proteins were dissolved at a concentration of 2 mg/mL in running buffer (PBS) and 50 µL aliquots were chromatographed on a Superose^{TM} HR10/30 column using an ÄKTApurifier 10 system with a flow rate of 0.5 mL/min at 4 °C. Protein elution was recorded at 280 nm. The column was calibrated with the following molecular weight markers: Blue Dextran (M_r>2000), aldolase (M_r=158kDa), albumin (M_r=67kDa), ovalbumin (M_r=44kDa), chymotrypsinogen (M_r=25kDa), vitamin B12 (M_r=1,35kDa).

Protein preparation for SAXS.

Suspensions of ammonium sulfate precipitated material were first dialyzed against phosphate-buffered saline (PBS) containing 4 mM DTT and 20 mM lactose and then fractionated by gel filtration on a HiPrep 10/300 GL Superdex-75 column (GE Healthcare, Freiburg, Germany) equilibrated with 20 mM sodium/potassium phosphate pH 7.0 containing 150 mM sodium chloride and 4 mM β-mercaptoethanol, without and with 5 mM lactose in an ÄKTAprime system (GE Healthcare, Uppsala, Sweden). Protein containing fractions were concentrated to the final concentrations used in the experiments.

Small-angle X-ray scattering (SAXS).

SAXS data were collected on BM29 at the European Synchrotron Radiation Facility (ESRF, Grenoble, France) using the BioSAXS robot and a Pilatus 1M detector (Dectris AG, Baden-Daettwil, Switzerland) with synchrotron radiation at a wavelength of $\lambda = 0.1$ nm and a sample-detector distance of 2.867 m covering a q-range of 0.025 to 5 nm^{-1} [$q = 4\pi\sin(\theta)/\lambda$] where q is the momentum transfer, λ is the set wavelength and 2θ the scattering angle (4, 5). Each measurement consisted of 10 frames each of 1 s exposure of a 100 µL sample solution continuously flowing through a 1 mm diameter capillary. Buffer scattering was immediately determined before each measurement of the corresponding protein sample at 10 °C. The scattering images obtained were spherically averaged to give the final scattering profile, and the buffer scattering intensities subtracted using in-house software. A series of solutions of the different proteins were prepared at concentrations ranging from 2 to 10 mg/mL in 20 mM sodium/potassium phosphate buffer at pH 7.0 containing 150 mM NaCl, 4 mM β-mercaptoethanol in the absence and the presence of 5 mM lactose. The samples were centrifuged at 10,000 × g for 10 min at room temperature immediately before data acquisition. Data on variants are summarized in Table S2. Data points affected by aggregation, possibly induced by radiation damage, were excluded. Regularized indirect transforms of the scattering data were performed with the program GNOM (6) to obtain the radius of gyration (Rg) and P(r) functions of interatomic distances. The value of Rg was also determined from the angular coefficient of the low q region in Guinier plots using PRIMUSQT (7). MW based Porod volume were obtained by dividing the Porod volume estimated with DATPOROD (8) by 1.7 (Table S3). This 1.7 was taken to be a maximal ratio between the Porod volume and the molecular weight (9).

Three-dimensional bead models that fitted with the scattering data were generated *ab initio* using the programs GASBOR (11) and DAMMIN/DAMMIF (11,12). Multiple runs were performed to generate several independent bead model for each sample. These models were aligned using SUPCOMB (13), averaged using the DAMAVER (14), and spatially filtered using DAMFILT (15). All calculated bead models were very consistent with the scattering data as reflected by low χ^2 values, and the normalized spatial discrepancy (NSD) value for each ensemble was below 2, indicating good consistency between the individual bead models (Table S4). All graphics were made with the program PyMol (16).

HDX analysis

Using a solution with Gal-3 CRD or the two homodimeric variants without/with Lac incubated for 1 h at RT to reach equilibrium, the exchange was started by adding 10-times deuteration buffer (pD 7.9, pH 7.5; 20 mM potassium phosphate containing 97 mM NaCl in D_20). After six intervals of time from 0.5 min to 240 min ice-cold quenching buffer (100 mM potassium phosphate buffer containing 5 M guanidinium hydrochloride and 0.5 M Tris[2-carboxyethyl]phosphine hydrochloride in H_20, pH 2.4) was added at a 1:1 ratio and the proteins were processed, as described for C-GRIFIN (17). The online peptic digestion on a Porozyme-presenting pepsin cartridge (2.1 mm x 30 mm; Applied Biosystem, Foster City, USA) was performed at 15 °C, peptides then trapped and fractionated as described in detail in (17). Using the DYNAMX software (Waters), relative deuterium uptake was calculated.

Isothermal Titration Calorimetry

Both ligand and lectin were prepared in buffer containing 20 mM phosphate, 150 mM NaCl, and 10 mM β-mercaptoethanol (Thermo Fisher), pH 7.2. Purified lectins were dialyzed against buffer for approximately 72 hours at 4 °C with buffer changes every 12 hours. Calorimetric measurements were recorded using a PEAQ-ITC calorimeter (Malvern, Westborough, USA). A solution of 36.4 µL of the ligand was titrated as an initial and excluded injection of 0.4 µL, followed by 2 µL injections into the calorimetric cell containing 200 µL of lectin. Injections were performed every 150 seconds for a total of 19 injections, at 25 °C and 750 rpm. The thermodynamic analysis was performed using the MicroCal PEAQ-ITC analysis software and a fitted offset parameter was applied to each titration to account for potential background signal.

Determination of Fluorescein/Protein Molar Ratio (F/P)

The F/P molar ratio is defined as the ratio of moles of FITC to moles of protein in the conjugate (18). To determine the F/P ratio the FITC conjugates were dissolved in 100 mM carbonate-buffer (pH 9) and the absorbance measured at 280 nm (A_{280}) and 495 nm

(A_{495}). From these absorbance readings the F/P ratio was calculated with the following formulas:

$$F/P = \frac{A_{495} \times C}{A_{280} - (0.35 \times A_{495})}$$

With:

$$C = \frac{MW \times E^{0.1\%}{}_{280}}{389 \times 195}$$

MW: is the molecular weight of the protein

(0.35 x A_{495}) is the correction factor due to the absorbance of FITC at 495 nm

$E^{0.1\%}{}_{280}$ is the absorption at 280 nm of the protein at 1 mg/mL.

Growth Assay

Cells were seeded at an initial density of 10^4 cells/well in 96-well plates and kept for 16 h. Culture medium consisted of Eagle's minimal essential medium supplemented with 10% fetal calf serum (Thermo Fischer, Dreieich, Germany). Then galectin constructs were added to a concentration of 100 µg/mL. After further culturing for 48 h extent of cell proliferation was measured with a commercial kit (CellTiter 96; Promega). All galectins were tested under identical conditions in parallel.

Binding assays

Radioiodination of galectin constructs was carried out under activity-preserving conditions using carrier-free $Na^{125}I$ and Iodobeads as described (2, 19) and yielded the following specific activities: Gal-3—Gal-3: 201 KBq/µg; Gal-3—8S—Gal-3: 211 KBq/µg; Gal-3—8L—Gal-3: 195 KBq/µg; Gal-3—Gal-1: 217 KBq/µg; Gal-3—8S—Gal-1: 209 KBq/µg; Gal-1—Gal-3: 193 KBq/µg; Gal-1—8S-Gal-3: 226 KBq/µg; Gal-3NT/1: 189 KBq/µg.

Human neuroblastoma cells (SK-N-MC) were grown to confluency in 96-well tissue culture plates with Eagle's minimal essential medium supplemented with 10% fetal calf serum and then kept for 16 h in serum-free Eagle's minimal essential medium (100 µL/well) prior to exposing the cells to the radioiodinated galectins in medium containing 25 mM HEPES (pH 7.4) and 0.01% carbohydrate-free bovine serum albumin to minimize carbohydrate-independent binding. Quantitation of cell-associated radioactivity after an incubation period of 2 h at 37 °C and thorough washes were done in a liquid scintillation

counter (TRI-CARB 2900TR; Perkin-Elmer, Rodgau, Germany). Extent of carbohydrate-dependent binding was determined by controls using a mixture of 150 mM lactose and 0.5 mg ASF/mL (3).

Synthesis of Spacer LacdiNAc-1

Synthesis of 1-[2-{2-(2-azidoethoxy)ethoxy}ethyl] 2-acetamido-2-deoxy-β-D-galactosyl-(1→4)-2-acetamido-2-deoxy-β-D-glucopyranoside (7)

Results and Discussion

The chloroethylenglycol spacer was introduced into compound **1** using BF_3-etherate as promoter and the chloride subsequently substituted with sodium azide to give compound **3** as described by Kato et al. (20). Zemplen deacetylation (→**4a**) followed by treatment with dimethoxytoluene gave compound **4b**. Initially the benzylidene acetal in **4b** was reductively opened to give a 6-*O*-benzyl 3,4-diol acceptor, which was glycosylated with donor **5** as described by Ellervik and Magnusson (21). On a small scale good 4-*O*-regioselectivity was obtained in the coupling, but on a larger scale 3-*O*-linked disaccharide was also formed which lowered the yield and complicated purification, why it was decided to protect the 3-OH prior to glycosylation. Acetylation of **4b** (→**4c**) followed by benzylidene ring opening afforded acceptor **4**, which was coupled with donor **5** using DMTST as promoter to yield disaccharide **6** in above 60% yield, even on a 0.5 g scale. Removal of protection groups and formation of acetamides was then performed in four steps (six if counting acetylations as separate steps), the Troc group was removed by treatment with TBAF (22), since Zn reduction can also reduce the azido function, and the free amine acetylated to afford **7a**. The phtalimido group was removed by treatment with ethylene diamine, which after acetylation gave **7b**. Removal of the 6-*O*-benzyl group, without concomitant reduction of the azido group, was accomplished by treatment with a mixture of sodium bromate and dithiosulfate as described by the group of Unverzagt (23) to yield **7c**. Zemplen deacetylation then afforded target structure **7**. The synthesis comprises 11 steps from the precursors **1** and ***5*** with an overall yield of 11% (average 81%/step) and was optimized to allow synthesis of gram quantities of **7**.

Carbohydrate Synthesis: General Methods

Dry reaction solvents as CH_2Cl_2 and THF were obtained from a PureSolv-EN™ solvent purification system (Innovation Technology Inc). All other anhydrous solvents were used as purchased from Sigma-Aldrich in AcroSeal® bottles. All solvents for silica gel chromatography were purchased from Sigma-Aldrich and were analytical grade. All chemicals for synthesis were purchased from commercial suppliers (Apollo Scientific Ltd, Carbosynth Ltd, Fisher Scientific Ltd, Merck, Sigma-Aldrich Corp, VWR) and used without further purification. A methanolic solution of NaOMe (1M) was always freshly prepared before each deacylation reaction by adding Na (69 mg, 3 mmol) in dry MeOH (3 mL).

^1H (500 MHz), ^{13}C (126 MHz) NMR spectra were recorded at 25 °C on a Varian (500 MHz) NMR spectrometer in chloroform-d^1 ($CDCl_3$), water-d^2 (D_2O). ^1H NMR spectra were standardized against the residual solvent peak ($CDCl_3$, δ = 7.26 ppm; D_2O, δ = 4.79 ppm; or internal tetramethylsilane δ = 0.00 ppm). ^{13}C NMR spectra were standardized against the residual solvent peak ($CDCl_3$, δ = 77.16 ppm; CD_3OD, δ = 49.00 ppm).

High-resolution mass spectrometry (HRMS) experiments were recorded on a Waters micromass LCT LC-Tof instrument using electrospray ionisation (ESI) in either the positive or negative mode. Low-resolution mass spectrometry (LRMS) experiments were recorded on a Waters micromass Quattro Micro LC-MS/MS instrument using electrospray ionisation (ESI) in either the positive or negative modes. Software for data acquisition and processing: MassLynx™ (version 4.0) (Water Micromass Ltd).

All reactions were monitored by thin-layer chromatography (TLC). TLC was performed on Merck TLC aluminum foil coated with a thickness of 0.2 mm silica gel 60 F254. Components were detected using ultraviolet light, followed 8% H_2SO_4 dip (stock solution: 8 mL conc. H_2SO_4, 92 mL EtOH) for visualizaiton.

Silica gel flash chromatography was carried out using *Davisil LC60A* (40-63 μm) silica gel. Solvent mixtures are expressed as ratios (v/v).

Deprotected sugars were lyophilised using a freeze-dryer Alpha 1-2 LDplus (Christ Ltd). Pressure: 0.035 mbar. Ice condenser temperature: -55 °C.

1-[2-{2-(2-Chloroethoxy)ethoxy}ethyl] 3,4,6-tri-*O*-acetyl-2-deoxy-2-phthalimido-β-D-glucopyranoside (2).

A solution of **1** (2.0 g, 4.55 mmol) and 2-[2-(2-chloroethoxy)ethoxy]ethanol (1.32 mL, 5.46 mmol) in dry CH_2Cl_2 (15 mL) containing freshly activated 3Å molecular sieves was stirred for 1 h at room temperature under N_2. The reaction mixture was then cooled to 0 °C, and TMSOTf (1 mL) was added. The reaction mixture was stirred at 0 °C for 24 h, and then filtered over a Celite pad. The filtrate was diluted with EtOAc (200 mL), and the solution was washed with saturated $NaHCO_3$ and brine. The organic layer was dried with $MgSO_4$, filtered and concentrated under reduced pressure. Purification by silica gel chromatography (cyclohexane/EtOAc 1:1) afforded compound **2** (1.92 g, 78% yield) as a white solid. **2**: $\mathbf{R}_f$ 0.3 (cyclohexane/EtOAc 1:1). **^{1}H NMR** (500 MHz, $CDCl_3$): δ 7.86 (m, 2H, ArH), 7.75 (m, 2H, ArH), 5.81 (dd, 1H, J = 10.4, 8.8 Hz, H-3), 5.44 (d, 1H, J = 8.4 Hz, H-1), 5.18 (dd, 1H, J = 10.0, 9.2 Hz, H-4), 4.33 (dd, 1H, J = 12.4, 4.8 Hz, H-6a), 4.33 (dd, 1H, J = 8.4, 10.4 Hz, H-2), 4.18 (dd, 1H, J = 12.4, 2.4 Hz, H-6b), 3.94 -3.86 (m, 2H, Glc-OC$\underline{H}_2$, H-5), 3.73 -3.68 (m, 1H, Glc-OC$\underline{H}_2$), 3.63 - 3.47 (m, 6H, O-CH_2CH_2-O), 3.43 - 3.35 (m, 4H, O-CH_2CH_2-O, C$\underline{H}_2$-Cl), 2.12 (s, 3H, C$\underline{H}_3$CO), 2.04 (s, 3H, C$\underline{H}_3$CO), 1.87 (s, 3H, C$\underline{H}_3$CO). **^{13}C NMR** (126 MHz, $CDCl_3$):170.92 (C$\underline{O}$$CH_3$), 170.32 (C$\underline{O}$$CH_3$), 169.72 (C$\underline{O}$$CH_3$), 167.61 (CO Phth), 134.50 (ArCH Phth), 131.61 (ArC Phth), 123.83 (ArCH Phth), 98.30 (C-1), 72.01 (C-5), 71.47 (C-3), 70.61 (O-CH_2CH_2-O), 70.55 (O-CH_2CH_2-O), 70.22 (O-CH_2CH_2-O), 69.34 (Glc-O$\underline{C}H_2$), 69.25 (C-4), 62.22 (C-6), 54.8 (C-2), 42.9 ($\underline{C}H_2$-Cl), 21.01 ($\underline{C}H_3$CO), 20.82 ($\underline{C}H_3$CO), 20.63 ($\underline{C}H_3$CO). **HRMS** $[M+Na]^+$ m/z calcd. for $C_{26}H_{32}ClNO_{12}Na$ 608.1511, found: 608.1480.

1-[2-{2-(2-Azideethoxy)ethoxy}ethyl] 3,4,6-tri-*O*-acetyl-2-deoxy-2-phthalimido-β-D-glucopyranoside (3).

Compound **2** (875 mg, 1.49 mmol) was dissolved in DMF (10 mL), and NaN_3 (394 mg, 5.97 mmol) was added to the solution. The reaction mixture was stirred for 16 h at 80 °C. Iced-water was added and the reaction mixture extracted with EtOAc. The organic phase was dried with $MgSO_4$, filtered, & concentrated. Purification by silica gel chromatography (cyclohexane/EtOAc 1:1) gave compound **3** (706 mg, 80% yield) as a

white solid. **Compound 3**: $\mathbf{R_f}$ 0.3 (cyclohexane/EtOAc 1:1). **^{1}H NMR** (500 MHz, $CDCl_3$): δ 7.88 (m, ArH phth), 7.76 (m, ArH phth), 5.84 (dd, 1H, *J* = 10.8, 8.7 Hz, H-3), 5.45 (d, 1H, *J* = 8.5 Hz, H-1), 5.19 (dd, 1H, *J* = 10.4, 9.2 Hz, H-4), 4.37 (dd, 1H, *J* = 8.4, 10.8 Hz, H-2), 4.34 (dd, 1H, *J* = 12.4, 4.8 Hz, H-6a), 4.19 (dd, 1H, *J* 12.4, 2.4 Hz, H-6b), 3.98 - 3.86 (m, 2H, Glc-OC$\underline{H}_2$, H-5), 3.73 -3.67 (m, 1H, CH, Glc-OC$\underline{H}_2$), 3.63-3.54 (m, 2H, O-$CH_2\underline{CH}_2$-O), 3.54-3.37 (m, 8H, O-$CH_2\underline{CH}_2$-O), 3.35 - 3.31 (m, 2H, CH, C$\underline{H}_2N_3$), 2.12 (s, 3H, C$\underline{H}_3$CO), 2.03 (s, 3H, C$\underline{H}_3$CO), 1.87 (s, 3H, C$\underline{H}_3$CO). **^{13}C NMR** (126 MHz, $CDCl_3$): 171.39 (C$\underline{O}$CH$_3$), 170.50 (C$\underline{O}$CH$_3$), 169.72 (C$\underline{O}$CH$_3$), 134.55 (ArCH Phth), 131.99 (ArC Phth), 123.79 (ArCH Phth), 98.50 (C-1), 72.07 (C-5), 70.95 (C-3), 70.72 (O-$CH_2\underline{CH}_2$-O), 70.57 (O-$CH_2\underline{CH}_2$-O), 70.32 (O-$CH_2\underline{CH}_2$-O), 69.38 (Glc-O$\underline{C}H_2$), 69.19 (C-4), 62.28 (C-6), 54.80 (C-2), 50.81 (-$\underline{C}H_2N_3$), 21.04 ($\underline{C}H_3$CO), 20.88 ($\underline{C}H_3$CO), 20.74($\underline{C}H_3$CO). **HRMS** $[M+Na]^+$ m/z calcd. for $C_{26}H_{32}N_4O_{12}Na$ 615.1914, found: 615.1928.

1-[2-{2-(2-Azidoethoxy)ethoxy}ethyl] 2-deoxy-2-phthalimido-β-D-glucopyranoside (4a).

Compound **3** (1.30 g, 2.21 mmol) was dissolved in MeOH (150 ml) at 0 °C. NaOMe (15 mg, 0.28 mmol) was added and the reaction kept stirring at room temperature for 16 h (TLC CH_2Cl_2/MeOH 9:1). The reaction mixture was neutralized with Dowex-50W (H^+) resin, filtered, and concentrated. The crude residue was dried under vacuum to give **4a** as a white foam which was used without any further purification in the next step. **4a**: $\mathbf{R_f}$ 0.4 (CH_2Cl_2/MeOH 9:1). **LRMS** $[M+Na]^+$ m/z calcd. for $C_{20}H_{26}N_4O_9Na$ 489.16, found: 488.99.

1-[2-{2-(2-Azidoethoxy)ethoxy}ethyl] 4,6-*O*-benzylidene-2-phthalimido-2-deoxy-β-D-glucopyranoside (4b).

Benzaldehyde dimethylacetal (0.68 ml, 4.63 mmol) and CSA (100 mg, 0.43 mmol) were added to a solution of **4a** (740mg, 1.58 mmol) in DMF (8 ml), and the mixture stirred at 60 °C. After 6 h (TLC CH_2Cl_2/MeOH 95:5) Et_3N was added to the solution until a pH of 7 was reached. The mixture was concentrated under reduced pressure and purified by silica gel chromatography (CH_2Cl_2/MeOH 97:3) to give compound **4b** (704 g, 80% yield, over two steps) as a white foam. **Compound 4b**: $\mathbf{R_f}$ 0.33 (CH_2Cl_2/MeOH 95:5). **^{1}H NMR** (500 MHz, $CDCl_3$) δ 7.86 (dd, *J* = 5.5, 3.0 Hz, 2H, ArH Phth), 7.73 (dd, *J* = 5.5, 3.0 Hz, 2H,

ArH Phth), 7.54 – 7.47 (m, 2H, ArH Ph), 7.37 (dd, *J* = 5.2, 2.0 Hz, 3H, ArH Ph), 5.57 (s, 1H, CHPh), 5.32 (d, *J* = 8.5 Hz, 1H, H-1), 4.65 (t, *J* = 9.4 Hz, 1H, H-3), 4.38 (dd, *J* = 10.5, 4.5 Hz, 1H, H-6a), 4.25 (dd, *J* = 10.5, 8.5 Hz, 1H, H-2), 3.90 (ddd, *J* = 11.3, 5.1, 3.5 Hz, 1H, Glc-OCH$_2$), 3.80 – 3.87 (m, 1H, H-6b), 3.70 – 3.66 (m, 1H, Glc-OCH$_2$), 3.66 – 3.58 (m, 2H, H-5, H-4), 3.56 – 3.43 (m, 4H, O-CH$_2$CH$_2$-O), 3.42 – 3.27 (m, 6H, O-CH$_2$CH$_2$-O, -CH$_2$N$_3$). **^{13}C NMR** (126 MHz, CDCl$_3$) δ 168.18 (CO Phth), 137.11 (ArC Ph), 134.22 (ArCH Phth), 131.86 (ArC Phth), 129.47 (ArCH Ph), 128.50 (ArCH Ph), 126.43 (ArCH Ph), 123.52 (ArCH Phth), 102.08 (CHPh), 99.12 (C-1), 82.37 (C-4), 70.67 (O-CH$_2$CH$_2$-O), 70.55 (O-CH$_2$CH$_2$-O), 70.26 (O-CH$_2$CH$_2$-O), 70.04 (O-CH$_2$CH$_2$-O), 69.30 (Glc-OCH$_2$), 68.81 (C-6), 68.67 (C-3), 66.24 (C-5), 56.69 (C-2), 50.72 (-CH$_2$N$_3$). **HRMS** $[M+Na]^+$ m/z calcd. for $C_{27}H_{30}N_4O_9Na$ 577.1910, found: 577.1880.

1-[2-{2-(2-Azidoethoxy)ethoxy}ethyl] 4,6-*O*-benzylidene-3-*O*-acetyl-2-phthalimido-2-deoxy-β-D-glucopyranoside (4c).

Compound **4b** (700 mg, 1.26 mmol) was dissolved in a mixture of pyridine (6 ml) and acetic anhydride (3 mL) and stirred at room temperature. After 2 h (TLC cyclohexane/EtOAc 1:1) the reaction mixture was concentrated under reduced pressure and co-evaporated with toluene several times. Purification by silica gel chromatography (cyclohexane/EtOAc 6:4) gave compound **4c** (699 mg, 93% yield) as a white foam. **4c**: R_f 0.48 (cyclohexane/EtOAc 1:1). **^{1}H NMR** (500 MHz, CDCl$_3$) δ 7.86 (q, *J* = 4.0, 3.5 Hz, 2H, ArH Phth), 7.74 (dd, *J* = 5.7, 2.9 Hz, 2H, ArH Phth), 7.43 – 7.49 (m, 2H, ArH Ph), 7.33 – 7.39 (m, 3H, ArH Ph), 5.87 – 5.93 (m, 1H, H-3), 5.54 (s, 1H, CHPh), 5.50 (d, *J* = 8.4 Hz, 1H, H-1), 4.41 (dd, *J* = 10.4, 4.5 Hz, 1H, H-6b), 4.30 (ddd, *J* = 10.4, 8.5, 0.6 Hz, 1H, H-2), 3.91 (dddd, *J* = 11.4, 5.2, 3.5, 0.7 Hz, 1H, Glc-OCH$_2$), 3.85 (dd, *J* = 10.3, 9.5 Hz, 1H, H-6a), 3.73 – 3.81 (m, 2H, H-4, H-5), 3.70 (ddd, *J* = 11.4, 6.8, 3.6 Hz, 1H, Glc-OCH$_2$), 3.58 – 3.63 (m, 1H, O-CH$_2$CH$_2$-O), 3.44 – 3.57 (m, 4H, O-CH$_2$CH$_2$-O), 3.29 – 3.42 (m, 5H, O-CH$_2$CH$_2$-O, -CH$_2$N$_3$), 1.90 (s, 3H, CH$_3$CO). **^{13}C NMR** (126 MHz, CDCl$_3$) δ 170.23 (COCH$_3$), 168.22 (CO Phth), 137.18 (ArC Ph), 134.37 (ArCH Phth), 132.02 (ArC Phth), 128.97 (ArCH Ph), 128.41 (ArCH Ph), 126.24 (ArCH Ph), 123.73 (ArCH Phth), 101.47 (CHPh), 98.94 (C-1), 79.53 (C-4), 71.23 (O-CH$_2$CH$_2$-O), 70.47 (O-CH$_2$CH$_2$-O), 70.19 (O-CH$_2$CH$_2$-O), 69.87 (O-CH$_2$CH$_2$-O), 69.74 (C-3), 69.42 (Glc-OCH$_2$), 68.66 (C-6), 66.12

(C-5), 55.45 (C-2), 50.64 (-$\underline{C}H_2N_3$), 20.71 ($\underline{C}H_3CO$). **HRMS** $[M+Na]^+$ m/z calcd. for $C_{29}H_{32}N_4O_{10}Na$ 619.2016, found: 619.2005.

1-[2-{2-(2-Azidoethoxy)ethoxy}ethyl] 3-*O*-acetyl-6-*O*-benzyl-2-phthalimido-2-deoxy-β-D-glucopyranoside (4).

$NaCNBH_3$ (402.7 mg, 6.34 mmol) was added, under N_2 at rt, to a solution of **4c** (630 mg, 1.06 mmol) in THF (5.7 mL) containing molecular sieves (4 Å, acid washed, 150 mg). After stirring for 1 h, the reaction mixture was cooled down to 0 °C and HCl in Et_2O (1M, 6 mL) was added dropwise over a period of 4 h. The reaction was then quenched by addition of Et_3N (1.0 ml), and the mixture filtered, concentrated, and coevaporated with MeOH several times. Purification by silica gel chromatography (toluene/EtOAc 3:7) gave compound **4** (492 mg, 78% yield) as a white foam. **4**: $\mathbf{R_f}$ 0.3 (cyclohexane/EtOAc 1:1). **^{1}H NMR** (500 MHz, $CDCl_3$) δ 7.87 – 7.82 (m, 2H, ArH Phth), 7.73 (dd, *J* = 5.5, 3.0 Hz, 2H, ArH Phth), 7.38 – 7.32 (m, 4H, ArH Ph), 7.32 – 7.28 (m, 1H, ArH Ph), 5.65 (dd, *J* = 10.7, 8.7 Hz, 1H, H-3), 5.41 (d, *J* = 8.4 Hz, 1H, H-1), 4.67 – 4.60 (m, 2H, CH_2Ph), 4.23 (dd, *J* = 10.8, 8.5 Hz, 1H, H-2), 3.97 – 3.86 (m, 1H, Glc-OC$\underline{H}_2$), 3.85 – 3.82 (m, 2H, H-6), 3.82 – 3.77 (m, 1H, H-5), 3.76 – 3.71 (m, 1H, H-4), 3.71 – 3.65 (m, 1H, Glc-OC$\underline{H}_2$), 3.57 – 3.46 (m, 4H, O-CH_2CH_2-O) 3.42 – 3.32 (m, 4H, O-CH_2CH_2-O), 3.30 (dd, *J* = 5.6, 4.5 Hz, 2H, -CH_2N_3), 1.93 (s, 3H, CH_3CO). **^{13}C NMR** (126 MHz, $CDCl_3$) δ 170.13 ($\underline{C}OCH_3$), 168.41 (CO Phth), 137.38 (ArC Ph), 134.69 (ArCH Phth), 128.90 (ArC Phth), 128.28 (ArCH Ph), 128.22 (ArCH Ph), 124.01 (ArCH Ph), 123.73 (ArCH Phth), 98.53 (C-1), 74.92 (C-4), 74.40 ($C\underline{H}_2Ph$), 74.03 (C-3), 71.57 (C-5), 71.08 (O-CH_2CH_2-O), 70.89 (O-CH_2CH_2-O), 70.70 (C-6), 70.56 (O-CH_2CH_2-O), 70.40 (O-CH_2CH_2-O), 69.48 (Glc-OC$\underline{H}_2$), 55.15 (C-2), 51.12 (-$\underline{C}H_2N_3$), 21.2 ($\underline{C}H_3CO$). **HRMS** calcd. for $C_{29}H_{34}N_4O_{10}Na$ [M+Na]+m/z = 621.2173, found: 621.2147.

1-[2-{2-(2-Azidoethoxy)ethoxy}ethyl] 3,4,6-tri-*O*-acetyl-2-(2,2,2-trichloroethoxycarbony-lamino)-2-deoxy-β-D-galactosyl-(1→4)-3,6-di-*O*-benzyl-2-phthalimido-2-deoxy-β-D-glucopyranoside (6).

0.1 mmol scale: A solution of **4** (50 mg, 0.09 mmol) and **5** (1.5 eq., 70.6 mg, 0.135 mmol) in dry CH_2Cl_2 (1.2 mL) containing molecular sieves (4 Å, 30.0 mg) was cooled down to -20 °C under N_2. After 1h, DMTST was added to the mixture and stirring continued for

another 2 h (TLC cyclohexane/EtOAc 1:1), where after Et_3N (5.0 mL) was added to the reaction mixture which was then concentrated under reduced pressure. Silica gel column chromatography (cyclohexane/EtOAc 4:6) of the residue afforded compound **6** (63.4 mg, 64% yield) as a white foam. *1.0 mmol scale*: To a solution of **4** (550.0 mg, 0.92 mmol) and **5** (1.5 eq., 721.7 mg, 1.38 mmol) in dry CH_2Cl_2 (13.0 mL) molecular sieves (4 Å, 300.0 mg) were added and then cooled down to -20 °C. After 1h, DMTST (2 eq., 475.3 mg, 1.84 mmol) was treated to reaction mixture and stirred for 4 hours. Et_3N (10.0 mL) was then added to the reaction mixture (TLC cyclohexane/ethyl acetate = 1:1, v/v), and then concentrated under reduced pressure. Purification by silica gel chromatography (cyclohexane/ EtOAc 4:6, v/v) gave compound **6** (595mg, 61% yield) as a white foam. **6**: $\mathbf{R_f}$ 0.44 (cyclohexane /EtOAc 4:6). **^{1}H NMR** (500 MHz, $CDCl_3$) δ 7.88 – 7.80 (m, 2H, ArH Phth), 7.73 (dd, *J* = 5.6, 2.9 Hz, 2H, ArH Phth), 7.54 – 7.43 (m, 4H, 4H, ArH Ph), 7.43 – 7.35 (m, 1H, ArH Ph), 5.75 – 5.63 (m, 1H, H-3), 5.37 (d, *J* = 8.5 Hz, 1H, H-1), 5.25 (dd, *J* = 3.4, 1.1 Hz, 1H, H-4'), 4.87 (d, *J* = 12.1 Hz, 1H, CH_2 Troc), 4.76 – 4.61 (m, 3H, H-3', C$\underline{H}_2$Ph), 4.42 (d, *J* = 12.2 Hz, 1H, CH_2 Troc), 4.32 (d, *J* = 8.4 Hz, 1H, H-1'), 4.24 (dd, *J* = 10.8, 8.5 Hz, 1H, H-2), 4.16 – 4.09 (m, 1H, N$\underline{H}$Troc), 4.09 – 3.96 (m, 3H, H-6', H-4), 3.92 (ddd, *J* = 11.3, 5.2, 3.7 Hz, 1H, Glc-OC$\underline{H}_2$), 3.80 (dd, *J* = 11.1, 2.9 Hz, 1H, H-6a), 3.69 (qd, *J* = 4.8, 2.7 Hz, 4H,CH_2-CH_2, Glc-C$\underline{H}_2$, H-6b), 3.66 – 3.60 (m, 2H, H-5, H-2'), 3.57 – 3.45 (m, 4H, O-CH_2CH_2-O), 3.43 – 3.36 (m, 4H, O-CH_2CH_2-O), 3.31 (dd, *J* = 5.6, 4.5 Hz, 2H, -C$\underline{H}_2N_3$), 2.09 (s, 6H, CH_3CO), 1.96 (s, 3H, CH_3CO), 1.87 (s, 3H, CH_3CO). **^{13}C NMR** (126 MHz, $CDCl_3$) δ170.57 (C$\underline{O}CH_3$), 170.34 (C$\underline{O}CH_3$), 170.25 (C$\underline{O}CH_3$), 170.23 (C$\underline{O}CH_3$), 153.96 (CO Phth), 137.72 (ArC Ph), 134.24 (ArCH Phth), 131.71 (ArC Phth), 129.31 (ArCH Ph), 129.18 (ArCH Ph), 128.76 (ArCH Ph), 123.58 (ArCH Phth), 100.52 (C-1'), 98.28 (C-1), 75.60 (C-4), 74.62 (C$\underline{H}_2$-Ph), 74.17 (C-5), 73.76 (CH_2 Troc), 70.89 (C-3), 70.75 (O-CH_2CH_2-O), 70.60 (O-CH_2CH_2-O), 70.52 (C-5'), 70.33 (O-CH_2CH_2-O), 70.14 (C-3'), 70.01 (O-CH_2CH_2-O), 69.01 (Glc-OC$\underline{H}_2$), 67.35 (C-6), 66.25 (C-4'), 61.16 (C-6'), 55.02 (C-2), 52.46 (C-2'), 50.70 (-C$\underline{H}_2N_3$), 29.71 (C$\underline{H}_3CO$), 20.82 (C$\underline{H}_3CO$), 20.74 (C$\underline{H}_3CO$), 20.67 (C$\underline{H}_3CO$). **HRMS** $[M+Na]^+$ m/z calcd. for $C_{44}H_{52}Cl_3N_5O_{19}Na$ 1082.2220, found: 1082.2247.

1-[2-{2-(2-Azidoethoxy)ethoxy}ethyl] 3,4,6-tri-*O*-acetyl-2-acetamido-2-deoxy-β-D-galactosyl-(1→4)-3-*O*-acetyl-6-*O*-benzyl-2-phthalimido-2-deoxy-β-D-glucopyranoside (7a).

TBAF (1M in THF) (1.7 mL, 1.7 mmol) was added at rt to a stirred solution of **6** (900 mg, 0.85 mmol) in dry THF (13 mL). After 6 h, the solvent was removed under reduced pressure and the residue dissolved in EtOAc (200 mL) and washed with saturated $NaHCO_3$ and brine. The organic phase was then dried with $MgSO_4$, filtered, and concentrated. The yellowish reside was dissolved in pyridine (20 mL) and treated with Ac_2O (10 mL) overnight (TLC EtOAc/acetone 95:5). The reaction mixture was then concentrated and the residue purified by silica gel chromatography (cyclohexane/EtOAc 1:9) to yield compound **7a** (583 mg, 74% yield) as a white foam. **7a**: $\mathbf{R_f}$ 0.56 (EtOAc/acetone 95:5). **^{1}H NMR** (500 MHz, $CDCl_3$) δ 7.84 (t, *J* = 4.4 Hz, 2H, ArH Phth), 7.73 (dd, *J* = 5.6, 2.9 Hz, 2H, ArH Phth), 7.54 – 7.42 (m, 4H, ArH Ph), 7.42 – 7.36 (m, 1H, ArH Ph), 5.73 (dd, *J* = 10.8, 9.0 Hz, 1H, H-3), 5.38 (d, *J* = 8.5 Hz, 1H, H-1), 5.26 (d, *J* = 3.4 Hz, 1H, H-4'), 5.03 (dd, *J* = 11.2, 3.4 Hz, 1H, H-3'), 4.88 – 4.76 (m, 2H, $C\underline{H}_2$Ph, Gal-N$\underline{H}$Ac), 4.61 (d, *J* = 8.3 Hz, 1H, H-1'), 4.50 (d, *J* = 12.1 Hz, 1H, $C\underline{H}_2$Ph), 4.29 – 4.20 (m, 1H, H-2), 4.11 – 3.99 (m, 3H,H-6', H-4), 3.91 (ddd, *J* = 11.2, 5.2, 3.8 Hz, 1H, Glc-O$C\underline{H}_2$), 3.81 – 3.65 (m, 6H, H-2', H-5', H-5, H-6, Glc-O$C\underline{H}_2$,), 3.57 – 3.46 (m, 4H, O-CH_2CH_2-O), 3.45 – 3.34 (m, 4H, O-CH_2CH_2-O), 3.34 – 3.29 (m, 2H, $C\underline{H}_2N_3$), 2.09 (d, *J* = 1.0 Hz, 3H, CH_3CO), 2.08 (d, *J* = 1.1 Hz, 3H, CH_3CO), 1.97 (d, *J* = 1.2 Hz, 3H, CH_3CO), 1.89 (s, 3H, CH_3CO), 1.79 (s, 3H, NHC$\underline{H}_3$CO). **^{13}C NMR** (126 MHz, $CDCl_3$) δ 170.55 ($\underline{C}OCH_3$), 170.35 ($\underline{C}OCH_3$), 170.31 ($\underline{C}OCH_3$), 170.24 ($\underline{C}OCH_3$), 170.03 ($\underline{C}OCH_3$), 138.11 (ArC Ph), 134.39 (ArCH Phth), 131.69 (ArC Phth), 128.95 (ArCH Ph), 128.82 (ArCH Ph), 128.54 (ArCH Ph), 123.59 (ArCH Phth), 100.14 (C-1'), 98.29 (C-1), 75.33 (C-4), 74.41 (C-5), 73.78 ($\underline{C}H_2$-Ph), 71.18 (C-3), 70.65 (O-CH_2CH_2-O), 70.56 (C-5'), 70.42 (O-CH_2CH_2-O), 70.20 (O-CH_2CH_2-O), 69.94 (C-3'), 69.00 (Glc-O$\underline{C}H_2$-), 67.64 (C-6), 66.47 (C-4'), 61.16 (C-6'), 55.03 (C-2), 51.68 (C-2'), 50.73 (-$\underline{C}H_2N_3$), 23.46 (NH$\underline{C}H_3$CO), 20.83 ($\underline{C}H_3$CO), 20.80 ($\underline{C}H_3$CO), 20.79 ($\underline{C}H_3$CO), 20.73 ($\underline{C}H_3$CO). **HRMS** $[M+Na]^+$ m/z calcd. for $C_{43}H_{53}N_5O_{18}Na$ 950.3282, found: 950.3303.

1-[2-{2-(2-Azidoethoxy)ethoxy}ethyl] 3,4,6-tri-*O*-acetyl-2-acetamido-2-deoxy-β-D-galactosyl-(1→4)-3-*O*-acetyl-6-*O*-benzyl-2-acetamido-2-deoxy-β-D-glucopyranoside (7b).

A solution of **7a** (650 mg, 0.7 mmol) and ethylene diamine (0.47 mL, 7.0 mmol) in ethanol (25.0 mL) was heated at 70 °C for 5 h (TLC CH_2Cl_2/MeOH 9:1). The solvent was then

removed and the residue coevaporated several times with acetonitrile to remove ethylene diamine. The crude was treated with pyridine (40 mL) and Ac_2O (20 mL) overnight at rt (TLC CH_2Cl_2/MeOH 9:1). The reaction mixture was concentrated under reduced pressure and coevaporated with toluene several times. Purification by silica gel chromatography (CH_2Cl_2/MeOH 95:5) afforded compound **7b** (513 mg, 85% yield) as a white foam. **7b**: $\mathbf{R_f}$ 0.48 (CH_2Cl_2/MeOH 9:1). **^{1}H NMR** (500 MHz, $CDCl_3$) δ 7.48 – 7.36 (m, 5H, ArH Ph), 6.35 (d, *J* = 9.6 Hz, 1H, NH), 5.29 – 5.20 (m, 1H, H-4'), 5.04 – 4.87 (m, 3H, H-3, H-3', NH), 4.79 (d, *J* = 12.0 Hz, 1H, C$\underline{H}_2$Ph), 4.61 (d, *J* = 8.3 Hz, 1H, H-1), 4.50 – 4.38 (m, 2H, H-1', C$\underline{H}_2$Ph), 4.16 – 4.03 (m, 3H, H-2, H-6'), 3.96 – 3.84 (m, 3H, H-4, Glc-OC$\underline{H}_2$-, H-2'), 3.84 – 3.74 (m, 2H, H-5', OCH_2-CH_2O), 3.74 – 3.57 (m, 9H, H-6, OCH_2-CH_2O, Glc-OC$\underline{H}_2$-,), 3.49 (dd, *J* = 5.8, 4.1 Hz, 3H, H-5, OC$\underline{H}_2$-N_3), 2.11 (s, 3H, CH_3CO), 2.07 (s, 3H, CH_3CO), 2.03 (s, 3H, CH_3CO), 1.97 (s, 3H, NHC$\underline{H}_3$CO), 1.96 (s, 3H, CH_3CO), 1.77 (s, 3H, NHC$\underline{H}_3$CO). **^{13}C NMR** (126 MHz, $CDCl_3$) δ 170.92 (C$\underline{O}$$CH_3$), 170.54 (C$\underline{O}$$CH_3$), 170.52 (C$\underline{O}$$CH_3$), 170.48 (C$\underline{O}$$CH_3$), 170.29 (C$\underline{O}$$CH_3$), 170.26 (C$\underline{O}$$CH_3$), 137.99 (ArC Ph), 128.86 (ArCH Ph), 128.60 (ArCH Ph), 128.45 (ArCH Ph), 102.48 (C-1'), 101.09 (C-1), 75.20 (C-4), 74.70 (C-5), 73.96 (C$\underline{H}_2$-Ph), 73.93 (C-3), 71.90 (O-CH_2CH_2-O), 70.98 (O-CH_2CH_2-O), 70.66 (C-5'), 70.47 (C-3'), 70.11 (O-CH_2CH_2-O)69.07 (Glc-OC$\underline{H}_2$-), 68.87 (O-CH_2CH_2-O), 68.36 (C-6), 66.62 (C-4'), 61.52 (C-6'), 53.94 (C-2), 51.33 (C-2'), 50.79 (-C$\underline{H}_2N_3$), 23.52 (NHC$\underline{H}_3$CO), 23.39 (NHC$\underline{H}_3$CO), 21.23 (C$\underline{H}_3$CO), 20.92 (C$\underline{H}_3$CO), 20.85 (C$\underline{H}_3$CO), 20.22 (C$\underline{H}_3$CO). **HRMS** $[M+Na]^+$ m/z calcd. for $C_{37}H_{53}N_5O_{17}Na$ 862.3334, found: 862.3387.

1-[2-{2-(2-Azidoethoxy)ethoxy}ethyl] 3,4,6-tri-*O*-acetyl-2-acetamido-2-deoxy-β-D-galactosyl-(1→4)-3-*O*-acetyl-2-acetamido-2-deoxy-β-D-glucopyranoside (7c).

Compound **7b** (860 mg, 1.02 mmol) was dissolved in EtOAc (13.5 mL) and a solution of $NaBrO_3$ (695 mg, 9.18 mmol) in water (10 mL) was added. To this well stirred two-phase system, an aqueous solution of $Na_2S_2O_4$ (710 mg, 8.16 mmol) in water (20 mL) was added dropwise over 10 min at rt and stirring was then continued for another 2 h. After completion of the reaction (CH_2Cl_2/MeOH 9:1) the mixture was diluted with EtOAc and washed with aq. sodium thiosulfate. The organic layer was dried with $MgSO_4$, filtered, concentrated, and purified by silica gel chromatography (CH_2Cl_2/MeOH 9:1) to give compound **7c** (661 mg, 86% yield) as a white foam. **7c**: $\mathbf{R_f}$ 0.3 (CH_2Cl_2/MeOH 9:1, v/v). **^{1}H NMR** (500 MHz,

$CDCl_3$) δ 6.50 (d, *J* = 9.3 Hz, 1H, NH), 6.43 (d, *J* = 9.7 Hz, 1H, NH), 5.30 (d, *J* = 3.3 Hz, 1H, H-4'), 5.16 (dd, *J* = 11.3, 3.3 Hz, 1H, H-3'), 5.12 (dd, *J* = 10.4, 8.8 Hz, 1H, H-3), 4.83 (d, *J* = 8.4 Hz, 1H, H-1), 4.69 (d, *J* = 8.5 Hz, 1H, H-1'), 4.17 – 3.96 (m, 6H, H-2, H-2', H-5', H-4, H-6a, H-6'a), 3.91 – 3.76 (m, 6H, H-6b, H-6'b, Glc-OC$\underline{H}_2$-, OCH_2-CH_2O), 3.69 (qt, *J* = 7.6, 2.7 Hz, 3H, OCH_2-CH_2O), 3.64 – 3.57 (m, 3H, OCH_2-CH_2O), 3.51 (td, *J* = 5.7, 4.0 Hz, 2H, OC$\underline{H}_2$-N_3), 3.44 (dt, *J* = 9.4, 2.7 Hz, 1H, H-5), 2.13 (s, 3H, CH_3CO), 2.10 (s, 3H, CH_3CO), 2.05 (s, 3H, CH_3CO), 1.99 (s, 3H, NHC$\underline{H}_3$CO), 1.97 (s, 6H, CH_3CO , NHC$\underline{H}_3$CO). **^{13}C NMR** (126 MHz, $CDCl_3$) δ 170.93 ($\underline{C}OCH_3$), 170.89 ($\underline{C}OCH_3$), 170.54 ($\underline{C}OCH_3$), 170.48 ($\underline{C}OCH_3$), 170.27 ($\underline{C}OCH_3$), 170.26 ($\underline{C}OCH_3$), 137.99 (ArC Ph), 128.86 (ArCH Ph), 128.60 (ArCH Ph), 128.45 (ArCH Ph), 102.28 (C-1'), 101.84 (C-1), 75.79 (C-4), 75.20 (C-5), 74.45 (C-3), 71.72 (O-CH_2CH_2-O), 70.81 (O-CH_2CH_2-O), 70.50 (C-3'), 70.38 (C-5'), 70.06 (O-CH_2CH_2-O), 68.99 (Glc-O$\underline{C}H_2$-), 66.42 (C-4'), 61.29 (C-6), 60.69 (C-6'), 54.17(C-2), 51.29 (C-2'), 50.53 (-$\underline{C}H_2N_3$), 23.42 (NH$\underline{C}H_3$CO), 23.25 (NH$\underline{C}H_3$CO), 21.06 ($\underline{C}H_3CO$), 20.85 ($\underline{C}H_3CO$), 20.83 ($\underline{C}H_3CO$), 20.74 ($\underline{C}H_3CO$). **HRMS** $[M+Na]^+$ m/z calcd. for $C_{30}H_{47}N_5O_{17}Na$ 772.2865, found: 772.2881.

1-[2-{2-(2-Azidoethoxy)ethoxy}ethyl] 2-acetamido-2-deoxy-β-D-galactosyl-(1→4)-2-acetamido-2-deoxy-β-D-glucopyranoside (7).

0.1 mmol scale: To a solution of **7c** (45.0 mg, 0.06 mmol) in MeOH (2.0 mL) NaOMe was added to a pH of 10-12. The reaction mixture was stirred at rt for 4 h and then neutralized by addition of Dowex-50W (H^+) resin. The resin was filtered off and the filtrate concentrated. The residue was purified by C18 reversed phase silica gel chromatography (MeOH/H_2O 9:1-6:4) and lyophilized to give **7** (32.1 mg, 92% yield) as a white solid. *1.0 mmol scale*: To a solution of **7c** (615 mg, 0.82 mmol) in MeOH (10.0 mL) freshly prepared NaOMe was added to adjust a pH of 10-12. Reaction mixture was kept stirring at rt for 4 hours, followed by treatment with Dowex-50W (H^+) resin to neutralize. The crude was filtered with MeOH and removed the solvent under reduced pressure. The crude was purified by C18 reverse phase silica gel chromatography (MeOH/H_2O 9:1-6:4, v/v) and lyophilized to give **7** (420 mg, 88% yield) as a white solid. **7: ^{1}H NMR** (500 MHz, D_2O) δ 4.44 (d, *J* = 8.0 Hz, 1H, H-1), 4.40 (d, *J* = 8.4 Hz, 1H, H-1'), 3.88 (ddd, *J* = 11.7, 5.6, 3.0 Hz, 1H, Glc-OC$\underline{H}_2$-), 3.84 – 3.78 (m, 2H, H-4', H-2'), 3.73 (dd, *J* = 12.1, 2.2 Hz, 1H, H-6'a), 3.69 – 3.62 (m, 3H, Glc-OC$\underline{H}_2$-, H-6), 3.62 – 3.48 (m, 11H, O-CH_2CH_2-O, H-2', H-

3, H-4, H-5, H-6'b, H-3'), 3.42 – 3.36 (m, 3H, OC<u>H</u>$_2$-N$_3$, H-5'), 1.95 (s, 3H, <u>C</u>H$_3$CO), 1.92 (s, 3H, <u>C</u>H$_3$CO). **^{13}C NMR** (126 MHz, D$_2$O) δ 174.69 (<u>C</u>OCH$_3$), 174.43 (<u>C</u>OCH$_3$), 101.66 (C-1'), 100.90 (C-1), 79.06 (C-3), 75.26 (C-4), 74.46 (C-5), 72.54 (C-5'), 70.62 (C-3'), 69.64 (O-CH$_2$CH$_2$-O), 69.63 (O-CH$_2$CH$_2$-O), 69.53 (O-CH$_2$CH$_2$-O), 68.97 (Glc-OC<u>H</u>$_2$-), 67.54 (C-4'), 60.89 (C-6), 60.09 (C-6'), 54.75 (C-2), 52.48(C-2'), 50.07 (-<u>C</u>H$_2$N$_3$), 22.12 (<u>C</u>H$_3$CO). **HRMS** [M+Na]$^+$ m/z calcd. for $C_{22}H_{39}N_5O_{13}Na$ 604.2442, found: 604.2428.

JGD-LacdiNAc (9). To a mixed solution of 2-(3,4,5-tris(((methyl triethylene glycol)benzoyl)oxy))-2,2-bis-hydroxymethyl-3-oxo-prop2-yn-1-yl succinate (compound **8**, 320 mg, 0.182 mmol) in THF (20 mL) and **7** (97 mg, 0.182 mmol) in water (2 mL) was added CuSO$_4$·5H$_2$O (46 mg, 0.182 mmol) in water (2 mL), and sodium ascorbate (33 mg, 0.182 mmol) in water (2 mL), successively, under nitrogen atmosphere. The reaction mixture was allowed to stir at 23 °C for 24 h. The reaction mixture was concentrated to dryness. The crude product was further purified by silica column chromatography with a mobile phase of CH$_2$Cl$_2$/MeOH, 10:1 to 4:1 to yield compound **JGD-LacdiNAc** as a colorless gel (295 mg, 74%). Purity (HPLC): 99%+. ^{1}H NMR (500 MHz, CDCl$_3$) δ = 7.79 (s, 1H, 1×=*CH* (triazole)), 7.26 (s, 2H, 2×Ar*H*), 7.07 (s, 4H, 4×Ar*H*), 6.59 (s, 2H, 2×Ar*H*), 5.15 (br, 2H, 1×O-*CH$_2$*-TRZ), 4.83 (m, 6H, 3×*CH$_2$*), 4.52 (m, 4H), 4.18-4.23 (m, 6H), 3.47–3.89 (m, 60H) 3.34–3.35 (m, 9H, 3×O*CH$_3$*), 2.65 (br, 2H, 1×COO-*CH$_2$*CH$_2$CONH), 2.54 (br, 2H, COO-CH$_2$*CH$_2$*CONH), 2.03 (br, 3H, C*H$_3$*CNH), 1.87 (br, 3H, C*H$_3$*CNH), 1.71–1.77 (m, 8H, 4×-ArCH$_2$*CH$_2$*CH$_2$(CH$_2$)$_8$CH$_3$), 1.39–1.42 (m, 8H, 4×-ArCH$_2$CH$_2$*CH$_2$*(CH$_2$)$_8$CH$_3$), 1.25–1.30 (m, 64H, 4×-ArCH$_2$CH$_2$CH$_2$*(CH$_2$)$_8$*CH$_3$), 0.85–0.88 (t, *J* = 6.9 Hz, 12H, 4×-Ar(CH$_2$)$_{11}$*CH$_3$*). ^{13}C NMR (126 MHz, CDCl$_3$) δ = 173.1, 172.6, 172.2, 166.1, 165.8, 160.2, 152.3, 142.7, 142.4, 131.0, 124.8, 124.2, 109.1, 107.8, 106.6, 102.3, 101.4. 79.9, 75.5, 74.6, 72.9, 72.4, 71.9, 70.7, 70.6, 70.4, 70.2, 69.6, 69.4, 68.8, 68.3, 63.8, 61.2, 59.0, 59.0, 57.8, 55.4, 52.8, 50.2, 31.9, 31.2, 29.7, 29.7, 29.6, 29.4, 29.2, 26.1, 23.2, 22.7, 14.1. MALDITOF (m/z): [M+Na]$^+$ cald. for $C_{123}H_{206}N_6O_{38}Na$: 2,398.4; found 2,400.3.

Lac (**3-Lac**) and suLac (**3-suLac**)-presenting Janus glycodendrimers were prepared according to literature (24-26).

Preparation of nanoscale GDS by injection. A stock solution was prepared by dissolving the required amount of amphiphilic JGDs in THF. GDSs were then generated by injection of 100 μL of the stock solution into 2.0 mL PBS, followed by 5 s vortexing. Eppendorf Research Plus Single Channel Pipette (10 μL –100 μL) and VWR Signature Ergonomic High Performance Single-Channel Variable Volume Pipettor (100 μL – 1000 μL) were used for injection.

Dynamic light scattering (DLS). DLS was performed with a Malvern Instruments particle sizer (Zetasizer® Nano S, Malvern Instruments, UK) equipped with 4 mW He-Ne laser 633 nm and avalanche photodiode positioned at 175º to the beam and temperature-controlled cuvette holder. Instrument parameters were determined automatically along with measurement times. Experiments were performed in triplicate.

Cryogenic transmission electron microscopy (cryo-TEM). Cryo-TEM micrographs were taken on a Carl Zeiss Libra 120 Microscope (Oberkochen, Germany). Cryo-TEM samples were prepared by plunge freezing of aqueous dispersion on plasma-treated lacey grids. The vitrified specimens were transferred to a Gatan-910 cryo-holder. The images were recorded at a temperature of –170 °C with an acceleration voltage of 120 kV.

Aggregation assays. Aggregation assays of GDSs with lectins were monitored in semi-micro disposable cuvettes (path length, l = 0.23 cm) at 23 °C at wavelength λ = 450 nm by using a Shimadzu UV-*vis* spectrophotometer UV-1601 with Shimadzu/UV Probe software in kinetic mode. PBS solution of galectin (100 μL) was injected into PBS solution of GDSs (900 μL). The cuvette was shaken by hand for 1–2 s before data collection was started. The same solution of GDSs solution was used as a reference. PBS solutions of galectin were prepared before the agglutination assays and were maintained at 0 °C (ice bath) before data collection.

Supporting Figures

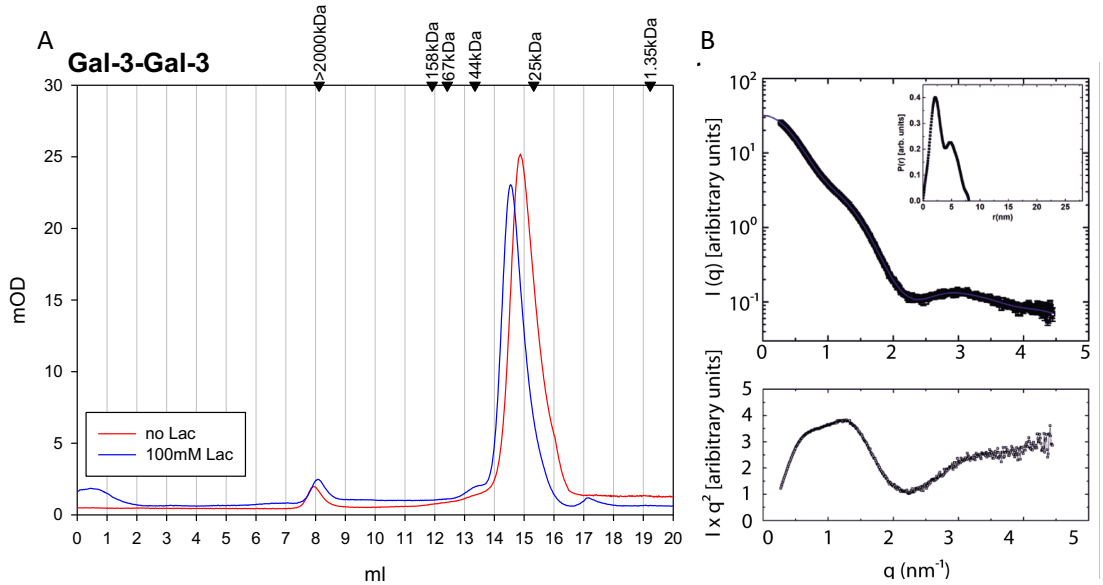

Fig. S1. Gel filtration (*A*) and scattering data (*B*) of the Gal-3–Gal-3.

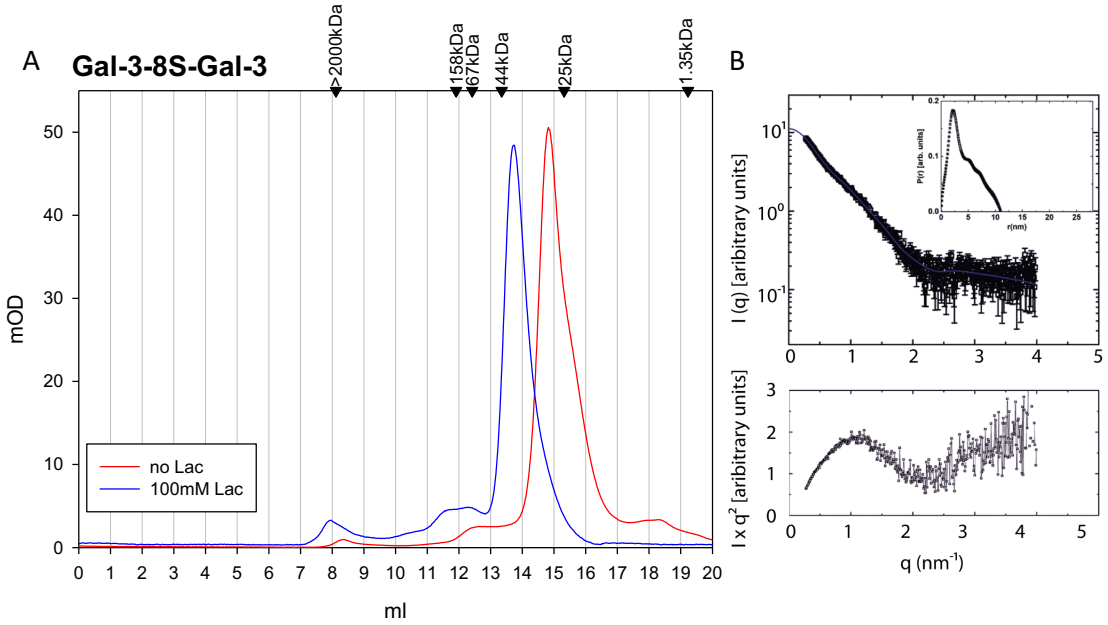

Fig. S2. Gel filtration (*A*) and scattering data (*B*) of the Gal-3–8S–Gal-3.

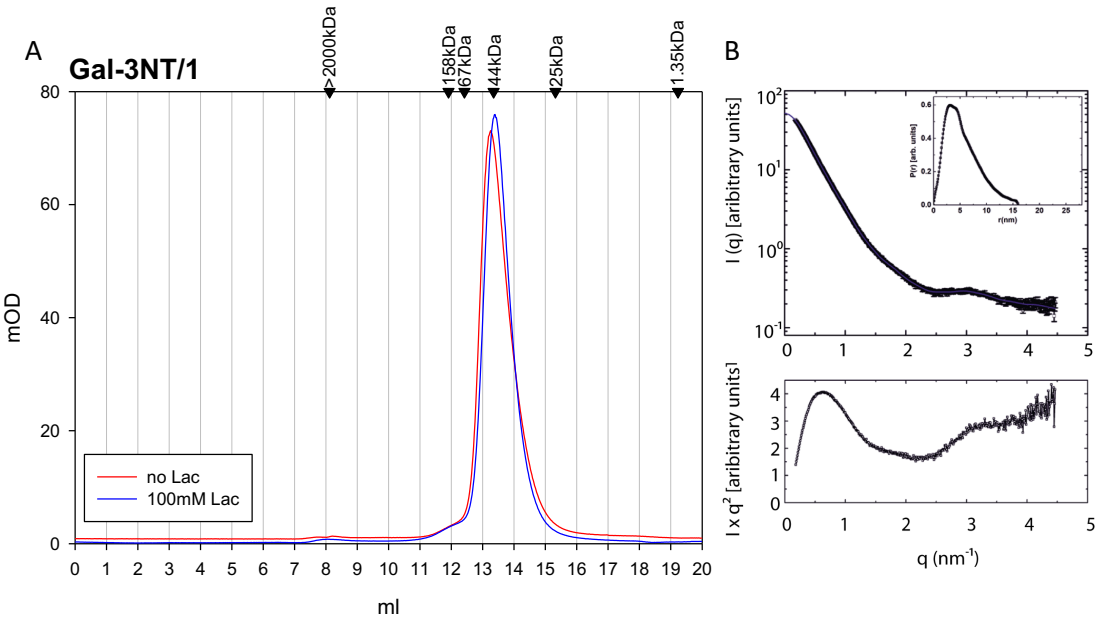

Fig. S3. Gel filtration (*A*) and scattering data (*B*) of the Gal-3NT/1.

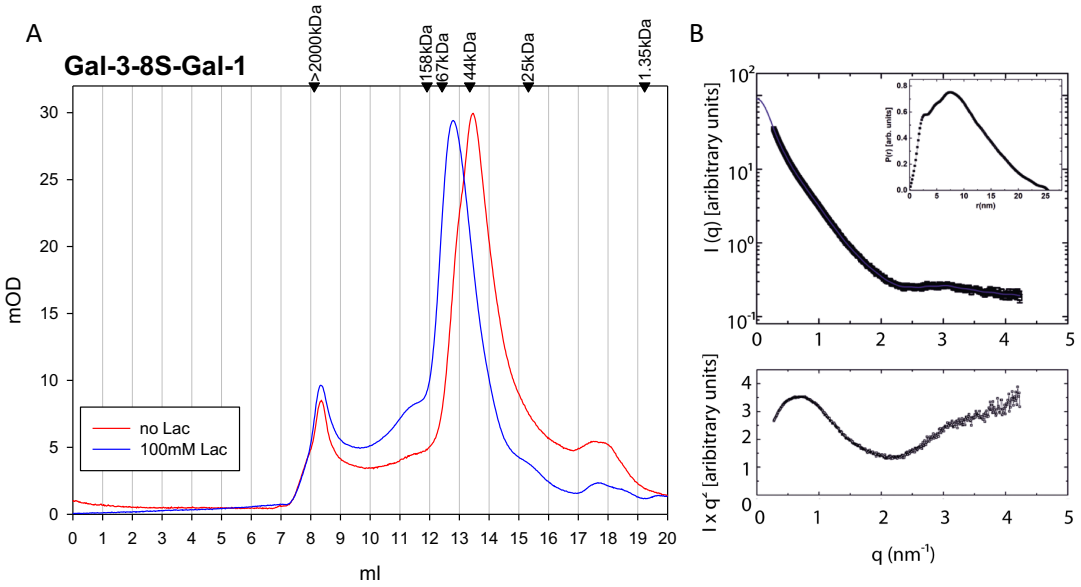

Fig. S4. Gel filtration (*A*) and scattering data (*B*) of the Gal-3–8S–Gal-1.

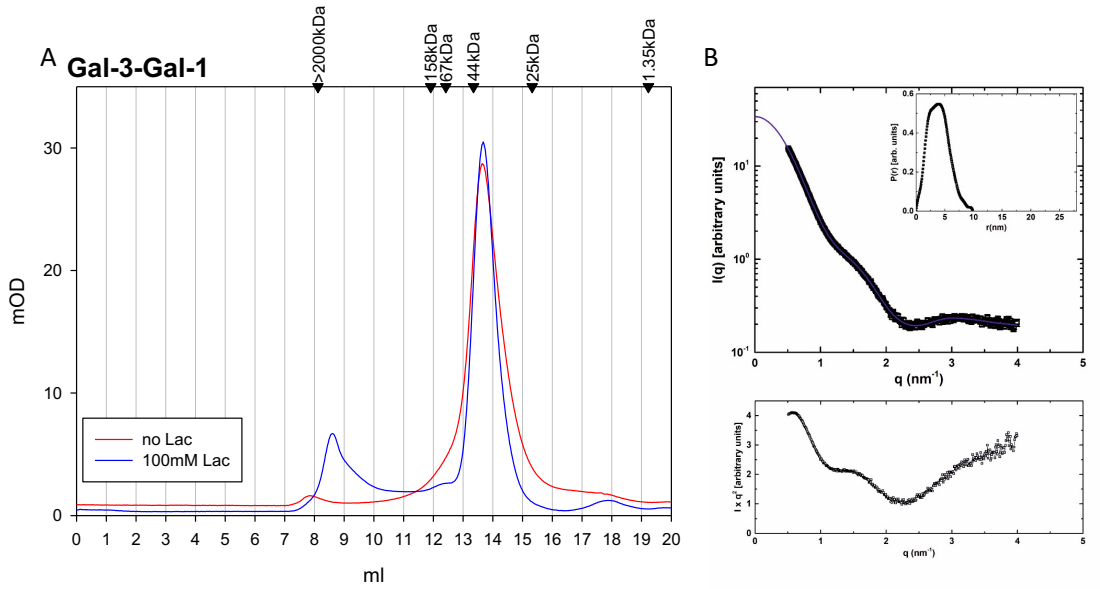

Fig. S5. Gel filtration (*A*) and scattering data (*B*) of the Gal-3–Gal-1.

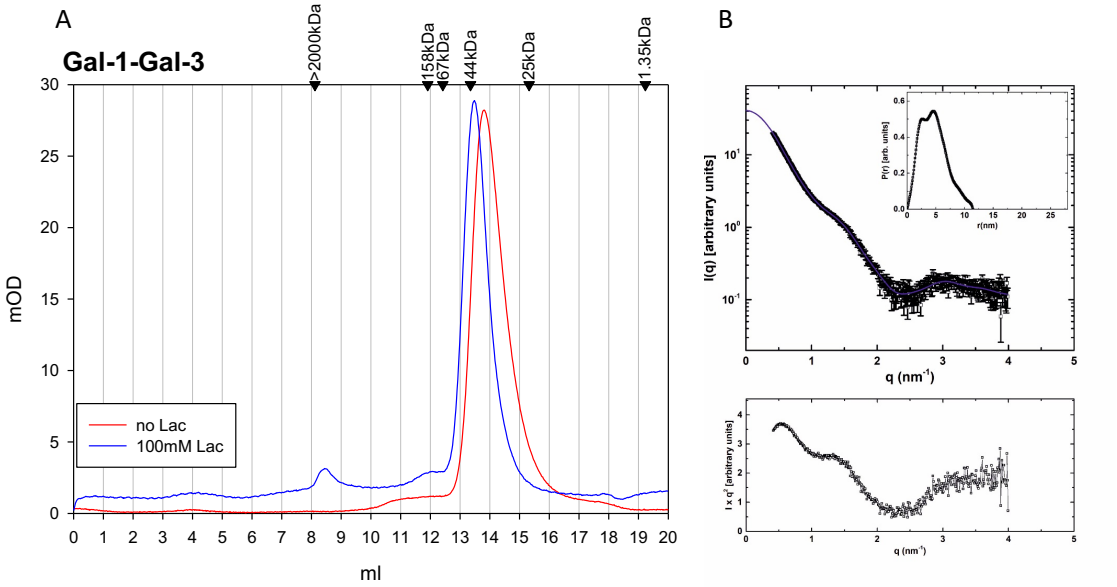

Fig. S6. Gel filtration (*A*) and scattering data (*B*) of the Gal-1–Gal-3.

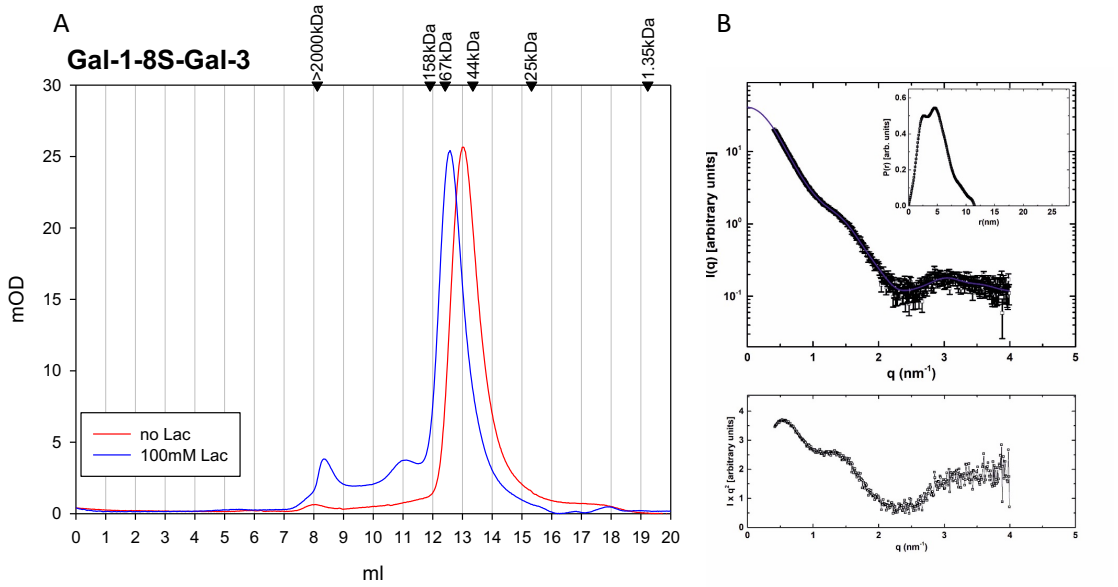

Fig. S7. Gel filtration (*A*) and scattering data (*B*) of the Gal-1–8S–Gal-3.

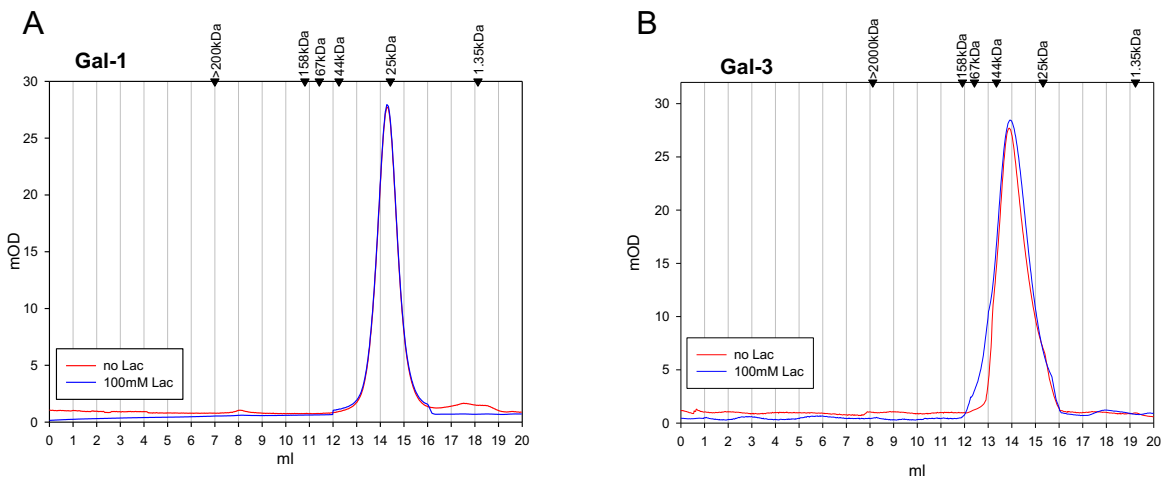

Fig. S8. Gel filtration of wild type galectins (A) Gal-1 and (B) Gal-3

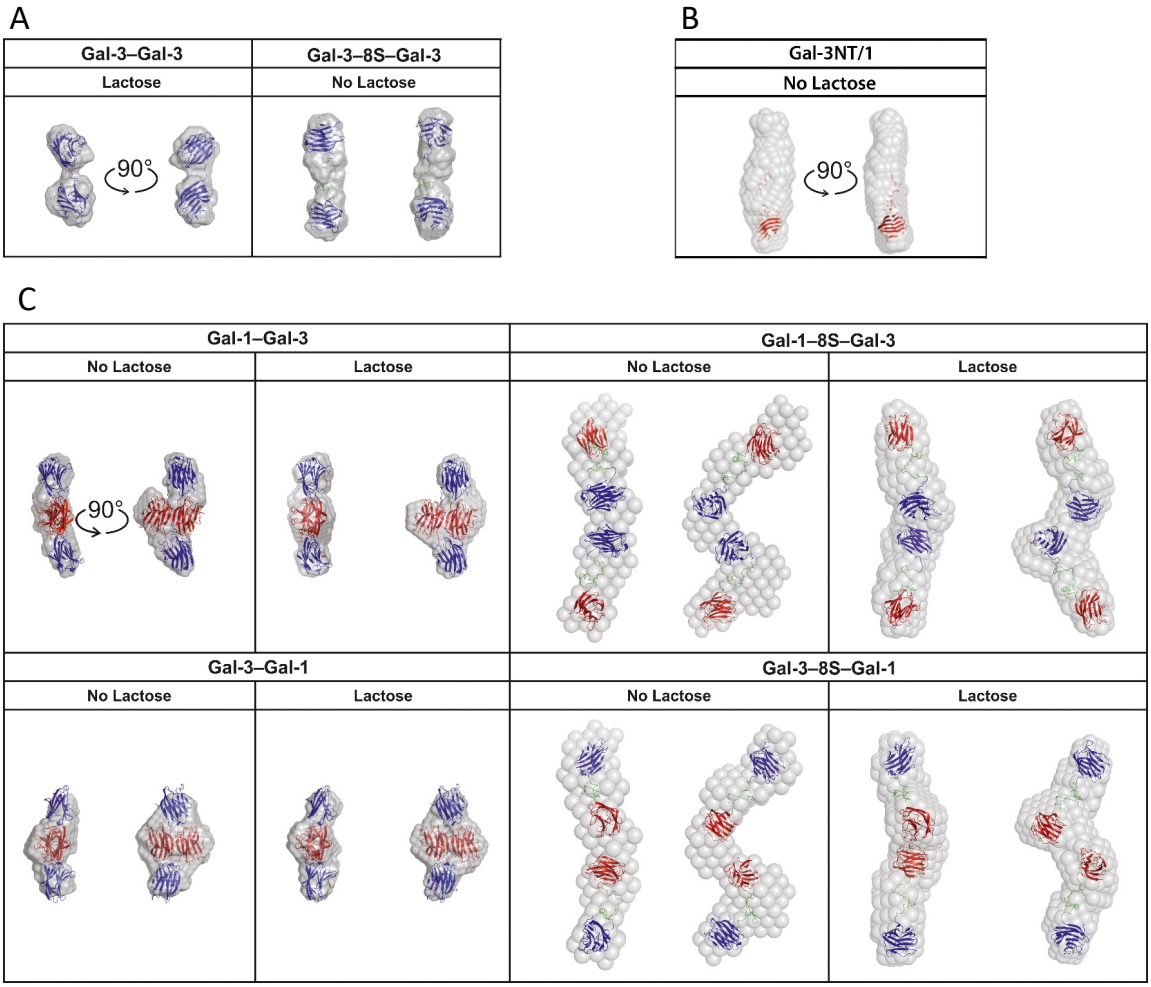

Fig. S9. Modelled structures of Gal-3–Gal-3 and Gal-3–8S–Gal-3 (blue cartoon, *A*), of Gal-3NT/1 (red cartoon, *B*) and of Gal-1–Gal-3, Gal-3–Gal-1, Gal-1–8S–Gal-3 and Gal-3–8S–Gal-1. All modelled structures are docked to the SAXS envelope (gray). The blue cartoon represents the structure of Gal-3, and the red cartoon that of Gal-1. The interaction between the monomers in Gal-1–8S–Gal-3 and Gal-3–8S–Gal-1 could not be determined with our data. Thus, here we represent two of the three possibilities, namely the interaction between the two Gal-3 units (Gal-1–8S–Gal-3) and the interaction between the two Gal-1 units (Gal-3–8S–Gal-1). The third possibility, the interaction between one unit of Gal-3 to one unit of Gal-1, is not shown.

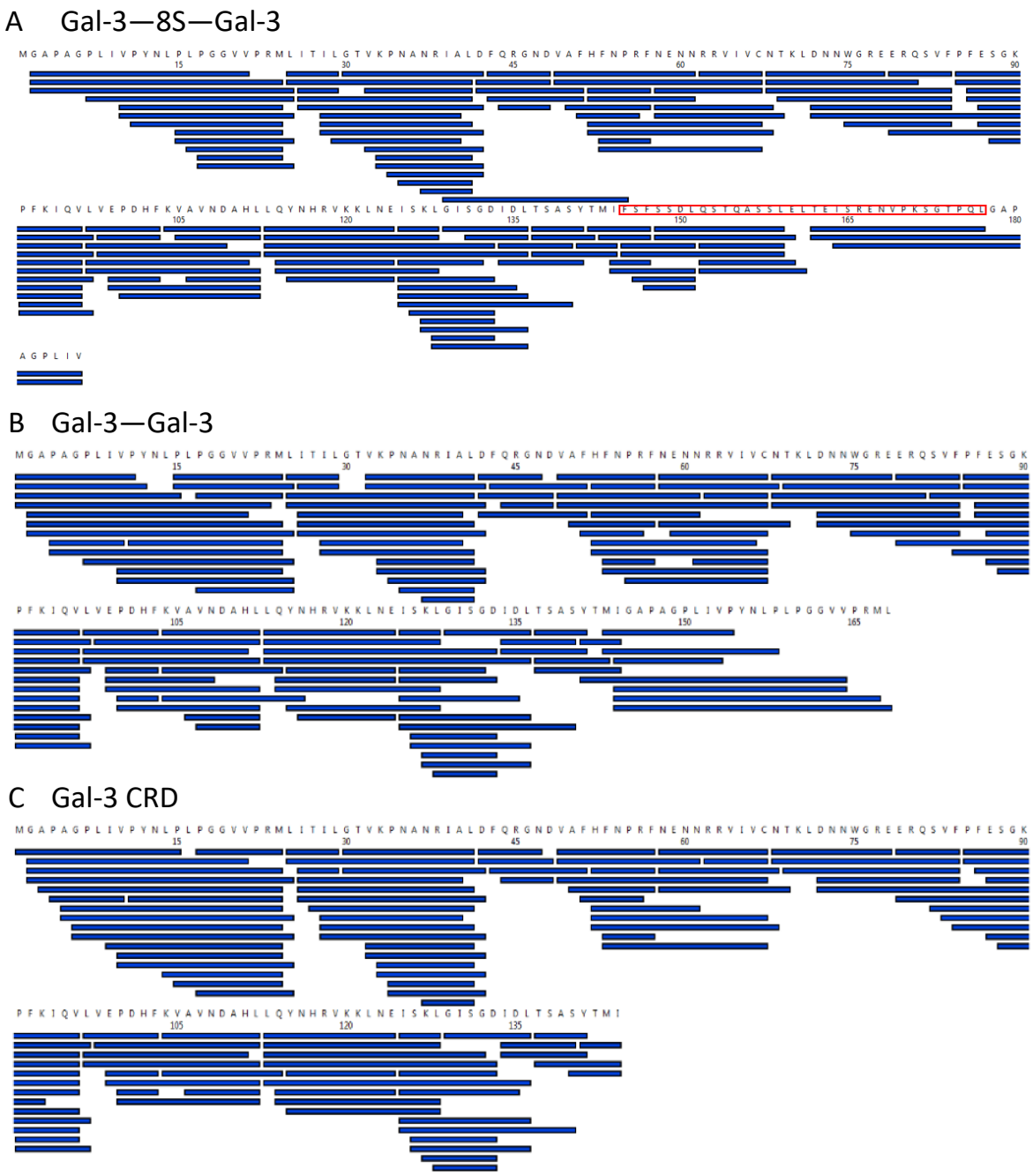

Fig. S10. Ligand binding of variants characterized by HDX revealing peptide-specific reduction of deuterium uptake (sequence coverage of peptides at redundancy of 7.32 for Gal-3–8S–Gal-3 (A), of 8.76 for the homodimer Gal-3–Gal-3 (B) and of 9.1 for Gal-3 CRD. The linker sequence in A is highlighted in red).

A Gal-3—8S—Gal-3

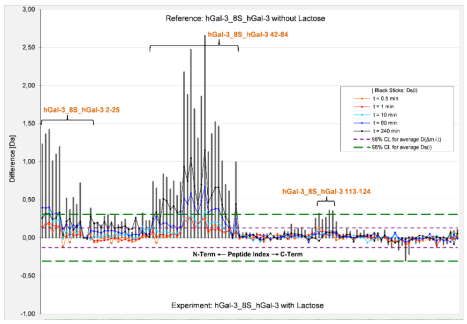

B Gal-3—Gal-3

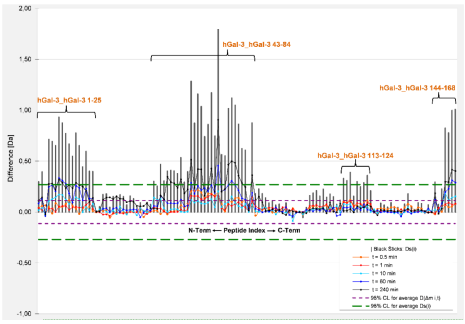

C Gal-3 CRD

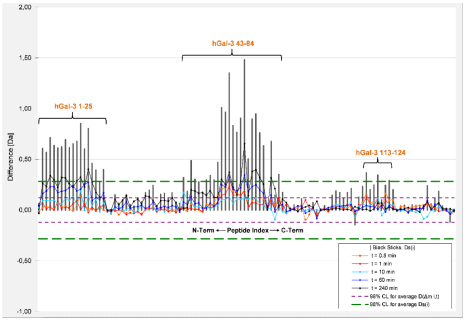

Fig. S11. Lac-dependent reduction of deuterium uptake for Gal-3–8S–Gal-3 (*A*), Gal-3–Gal-3 (*B*) and Gal-3 CRD (*C*).

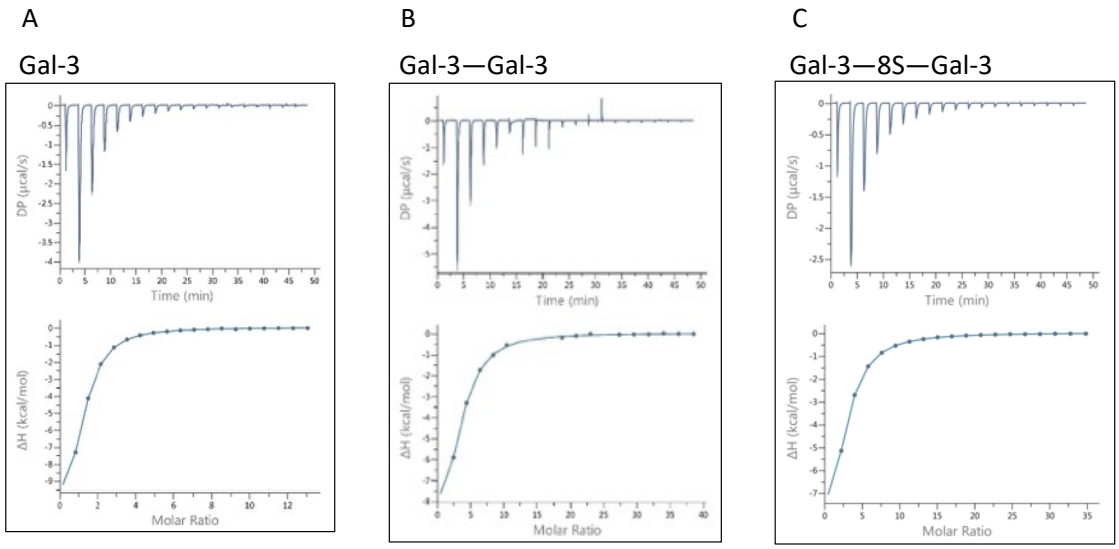

Fig. S12. ITC titration curves with LacNAc using WT Gal-3 (*A*), Gal-3–Gal-3 (*B*) and Gal-3–8S–Gal-3 (*C*), data summarized in Table 2.

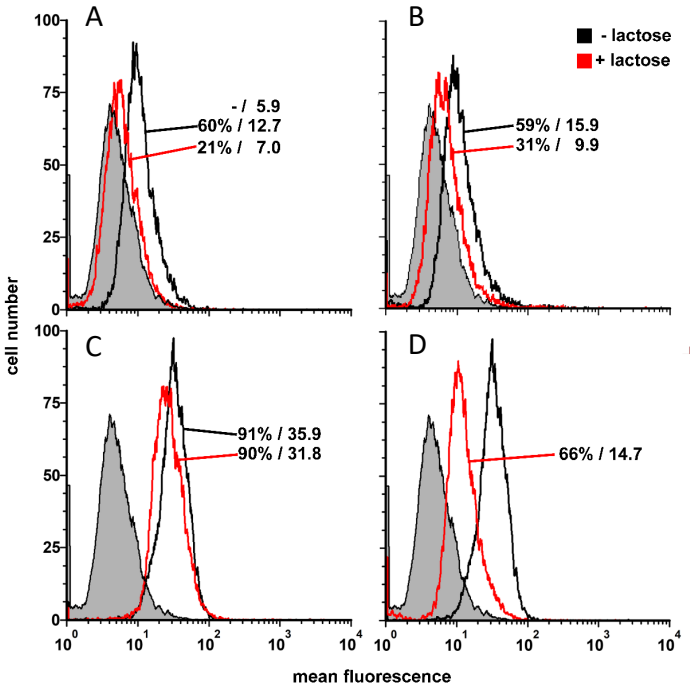

Fig. S13. Flow cytofluorimetric analysis of CHO WT cells using fluorescent WT Gal-3 (*A*, 10 μg/mL), Gal-3NT/1 (*B*, 5 μg/mL) and Gal-3—Gal-3 (*C*, *D*, 0.5 μg/mL) without Lac or in the presence of 10 mM Lac (*A*–*C*) or 50 mM (*D*). Numbers denote percentage of positive cells/mean fluorescence intensity.

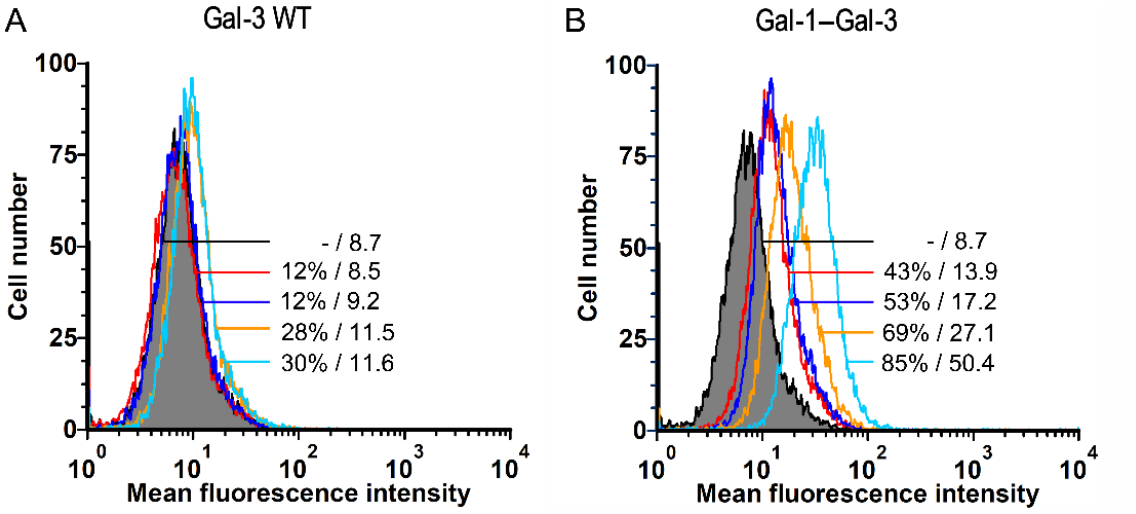

Fig. S14. Flow cytometric profiles of signal changes of staining of CHO Lec13 cells upon increasing probe concentration from 0.01 µg/mL to 0.1 µg/mL, 0.25 µg/mL and 0.5 µg/mL for the two given variants.

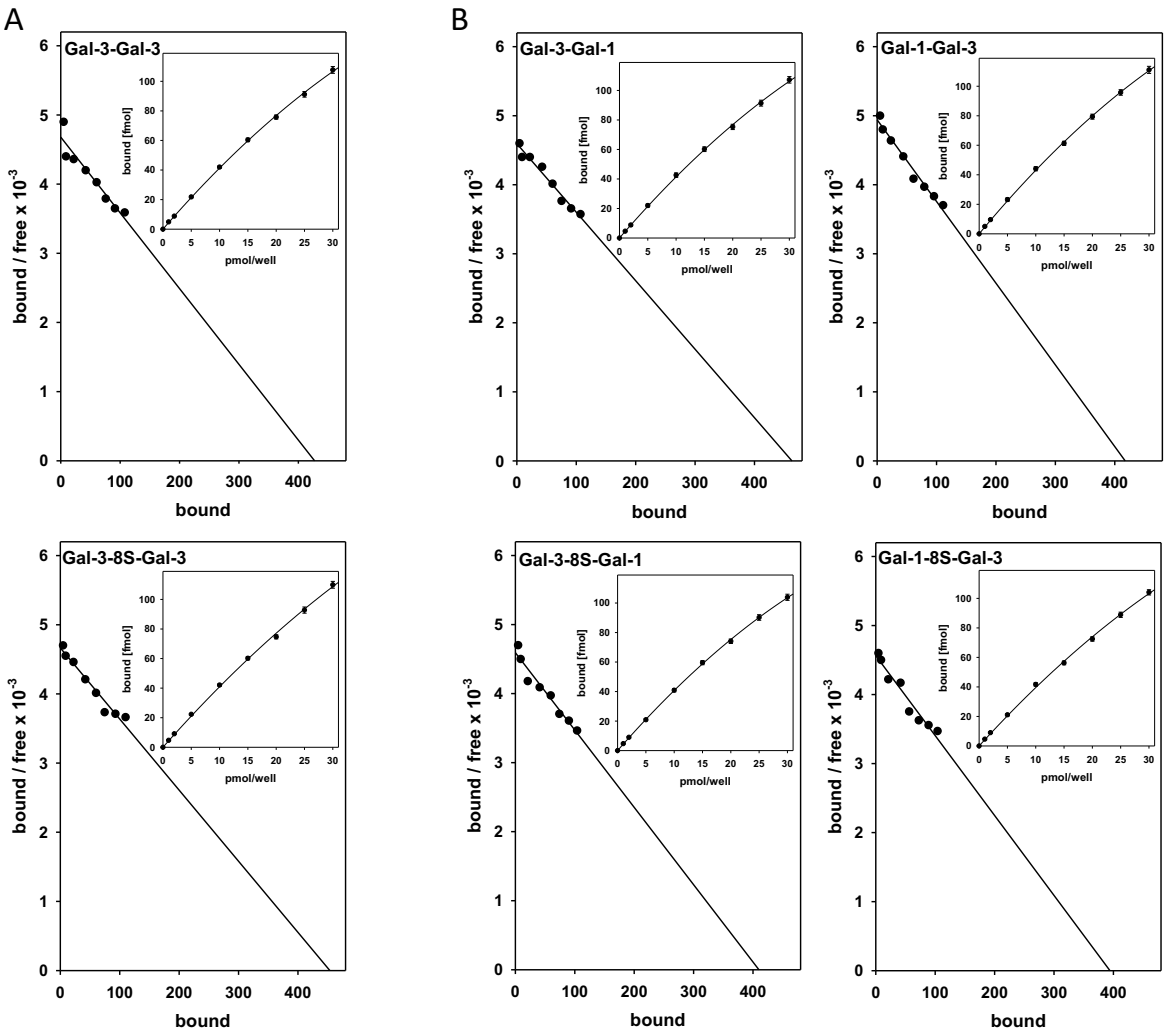

Fig. S15. Quantitation of binding of radioiodinated variants to the surface of human neuroblastoma (SK-N-MC) cells showing Scatchard plots and titration curves (inset) for the homodimers (*A*) and heterodimers (*B*) (please see also Table 2).

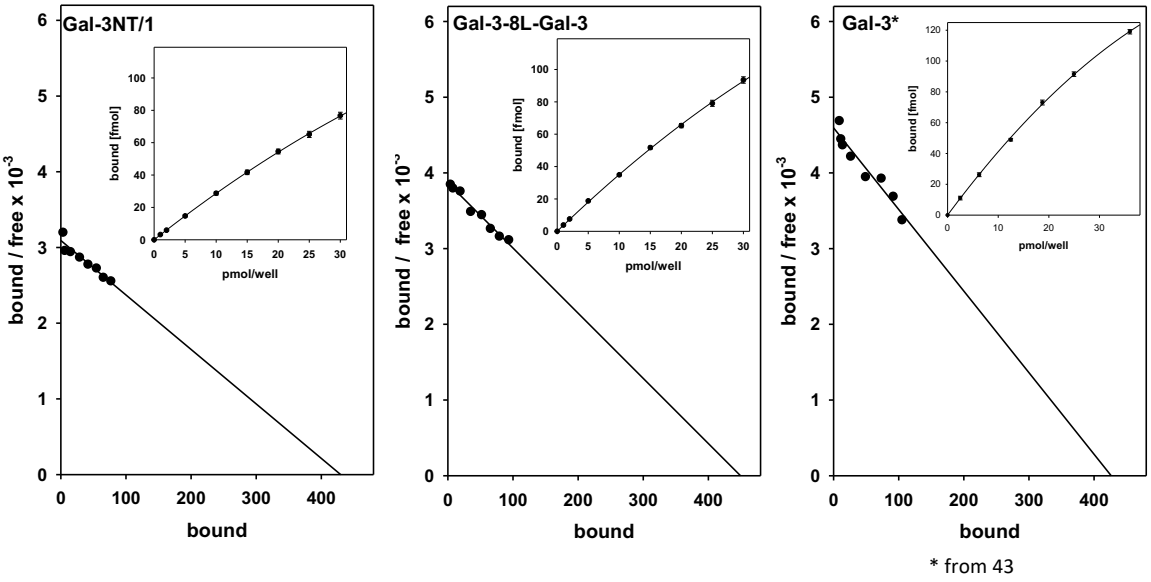

Fig. S16. Scatchard analysis and binding curves of specific association of radioiodinated galectins to the surface of human neuroblastoma (SK-N-MC) cells (please see also Table 2).

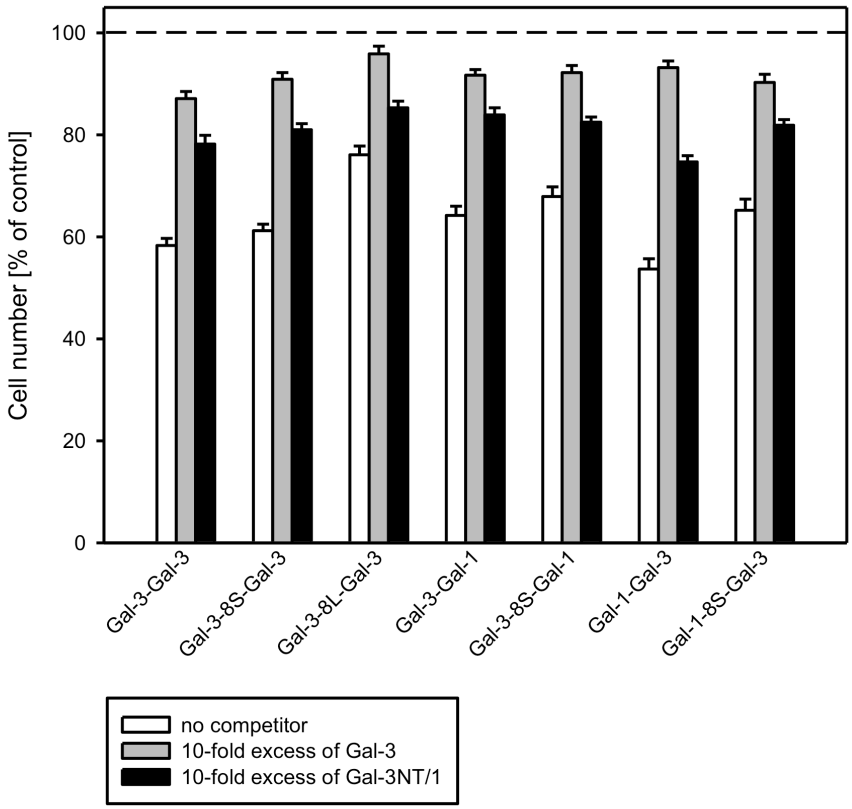

Fig. S17. Effect of presence of Gal-3 or Gal-3NT/1 (at 10-fold excess) on neuroblastoma cell growth inhibition by variant proteins. Values are means ± SD.

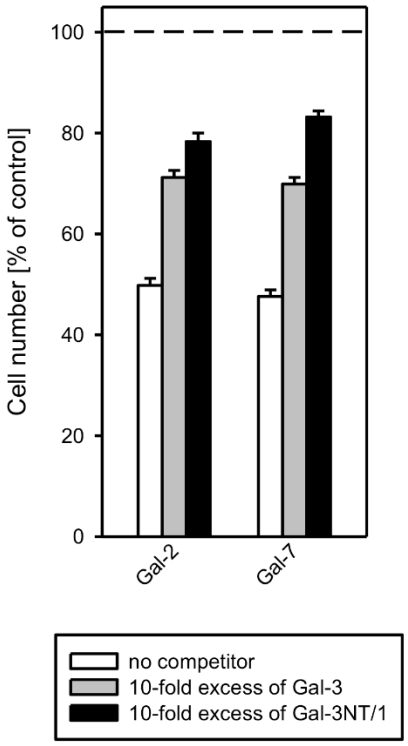

Fig. S18. Effect of presence of Gal-3 or Gal-3NT/1 (at 10fold excess) on neuroblastoma cell growth inhibition by galectin-2 or galectin-7. Values are means ± SD.

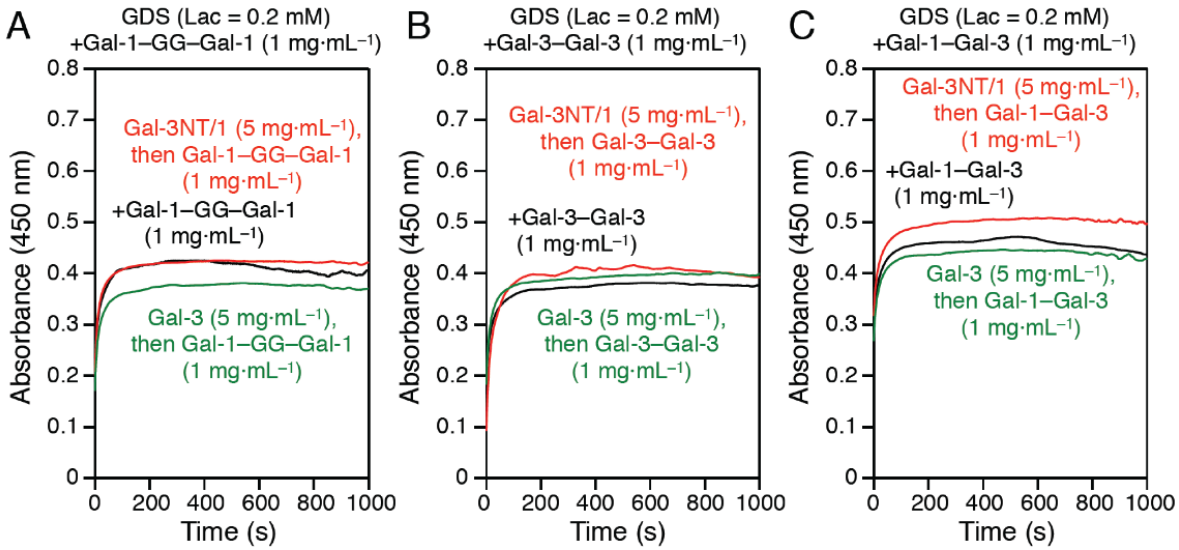

Fig. S19. Aggregation of Lac-presenting GDSs in the competitive mode (for comparison, please see Fig. 4*E*, *F*).

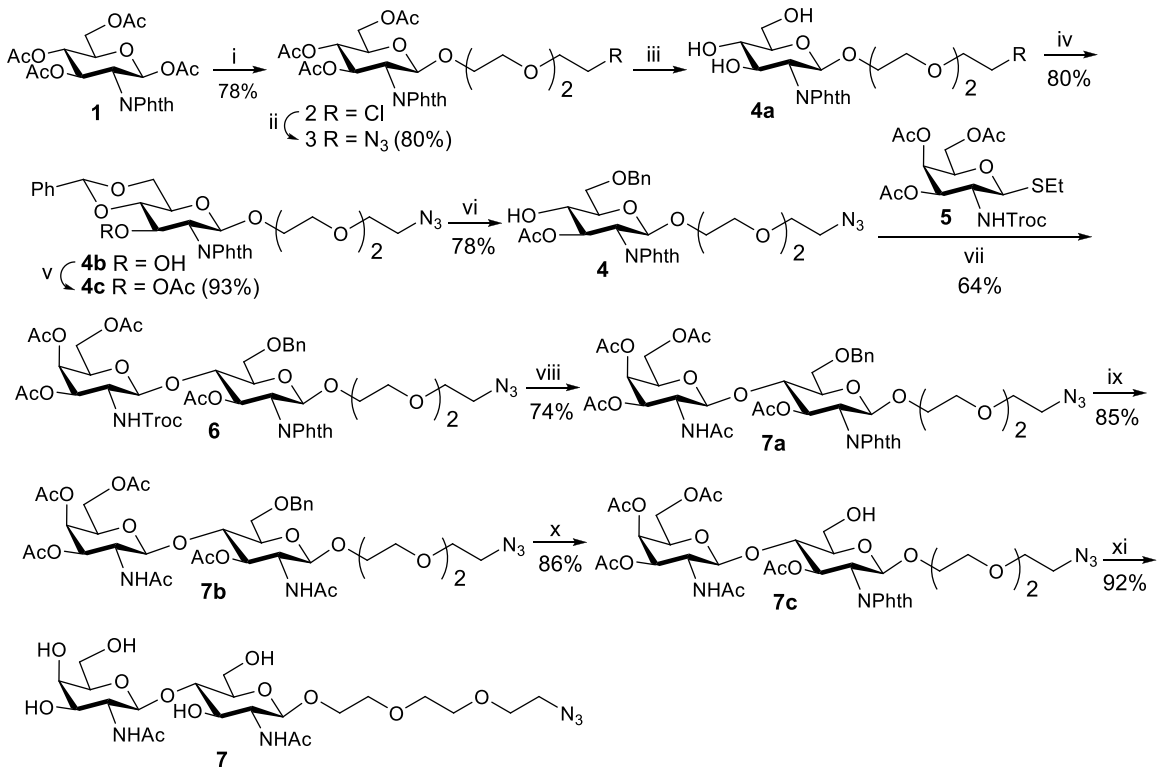

Fig. S20. Synthetic route to spacer LacdiNAc **7**. *Reagents and Conditions*: i. 2-[2-(2-chloroethoxy)ethoxy]ethanol, CH_2Cl_2, TMSOTf, 0 °C, 24 h; ii. NaN_3, DMF, 80 °C, 16 h; iii. MeOH, NaOMe, rt, 16 h; iv. DMF, $PhCH(OMe)_2$, CSA, 60 °C, 6 h; v. Ac_2O, Pyridine, 2 h; vi. HCl-AcOH, $NaCNBH_3$, THF, 0 °C, 4 h; vii. DMTST, CH_2Cl_2, MS 4Å, -20 °C; viii. a) TBAF, THF, rt, 6 h, b) Ac_2O, pyridine, rt, 16 h; ix. a) Ethylene diamine, EtOH, 70 °C, 5 h, b) Ac_2O, pyridine, 16 h; x. $NaBrO_3$, $Na_2S_2O_4$, EtOAc, rt, 2h; xi. MeOH, NaOMe, rt, 4 h.

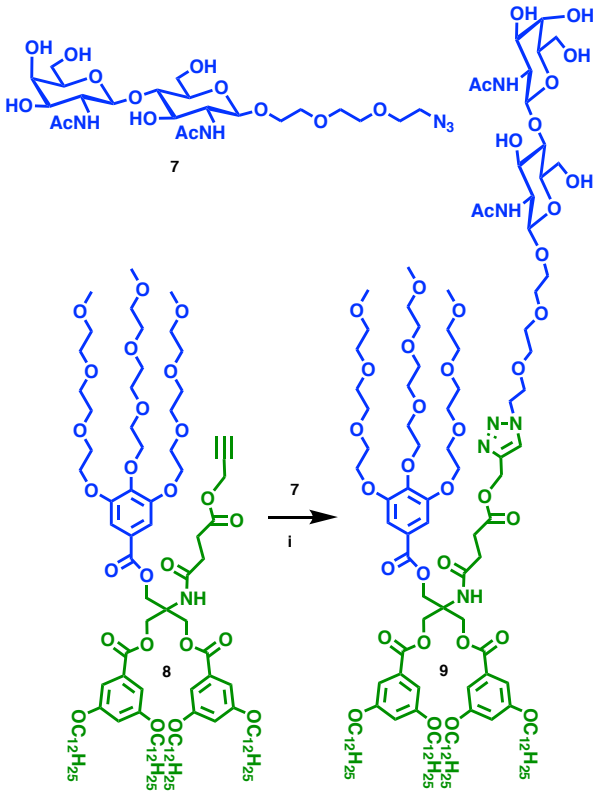

Fig. S21. Synthesis of LacdiNAc-presenting Janus GD. Reagents and conditions: *i*. $CuSO_4 \cdot 5H_2O$, sodium ascorbate, THF, water, 23 °C, 12 h, 74%.

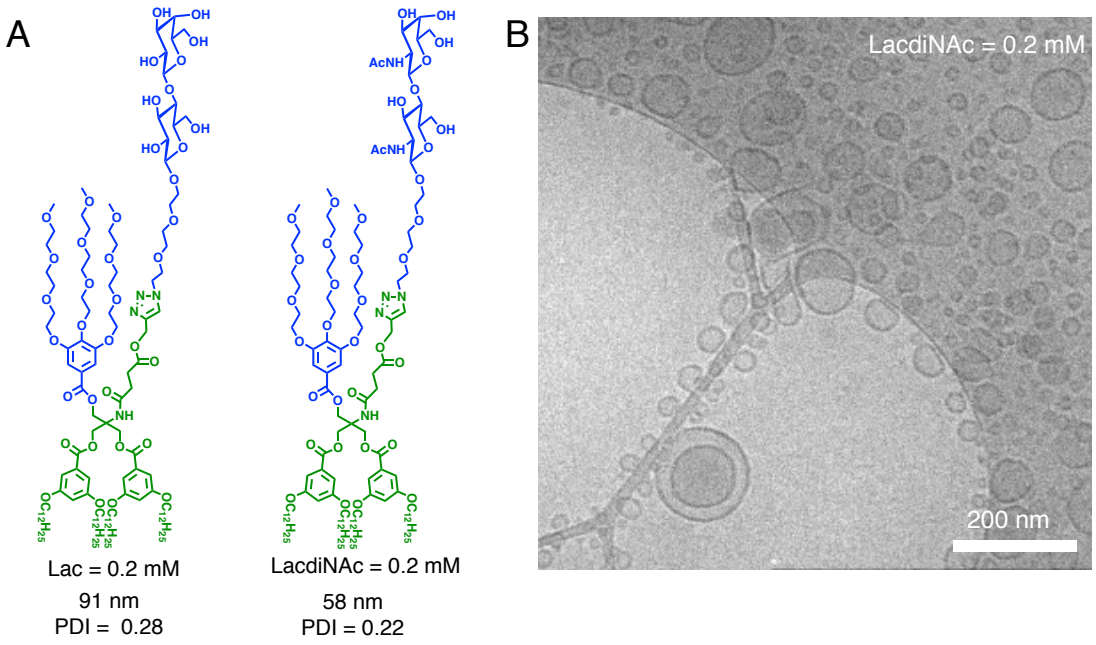

Fig. S22. Dynamic light scattering (DLS) data of the GDS size and polydispersity (PDI) for Lac- or LacdiNAc-presenting JGDs (*A*). Representative cryo-TEM image of the self-assembled GDS from LacdiNAc-presenting JGDs (*B*).

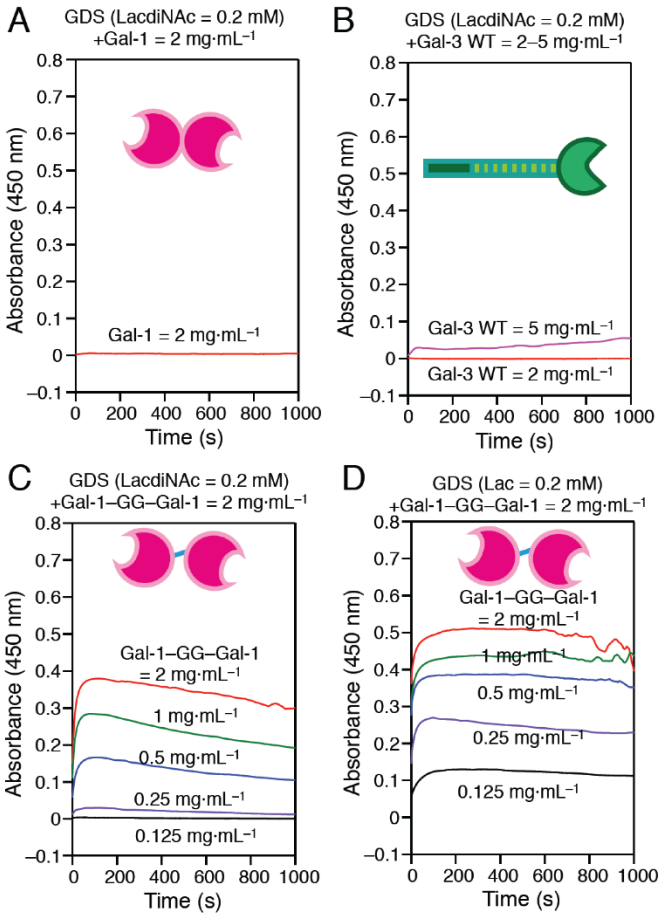

Fig. S23. Aggregation of LacdiNAc-presenting GDSs for WT Gal-1 (*A*), WT Gal-3 (*B*) and GG-linked Gal-1 homodimer (*C*) compared to this variant′s activity with Lac-presenting GDSs (*D*).

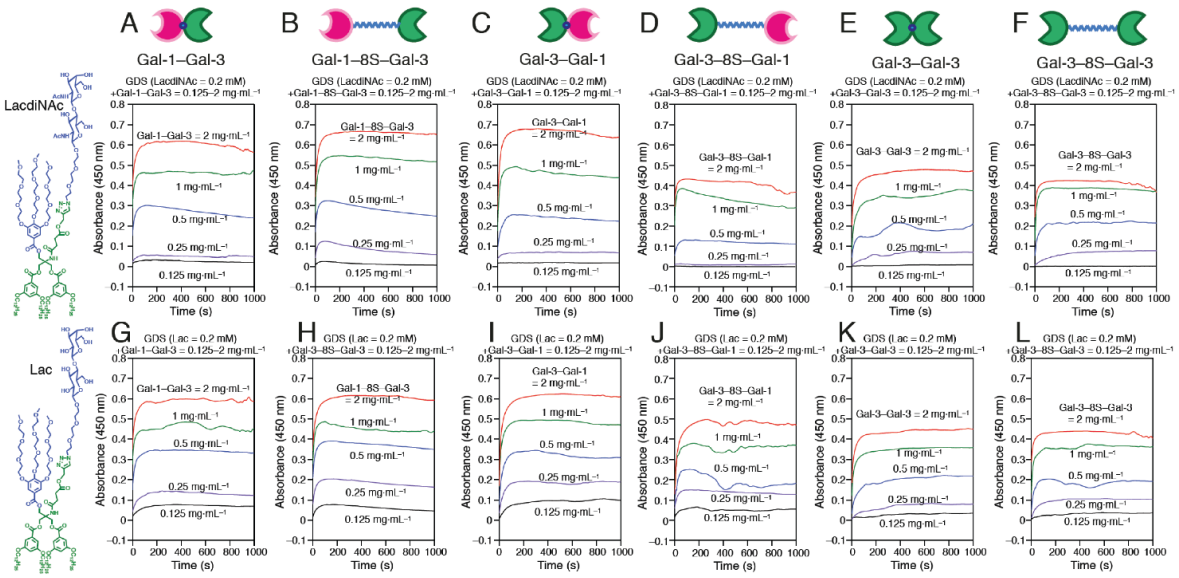

Fig. S24. Aggregation of Lac (*A–F*)-or LacdiNAc (*G–L*)-presenting GDSs by hetero- and homodimers (please see also Fig. 1*B*).

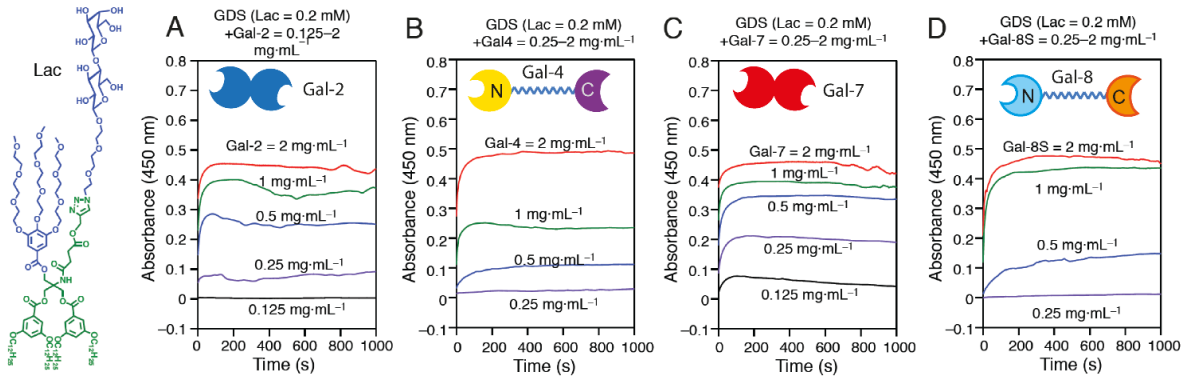

Fig. S25. Aggregation of Lac-presenting GDSs by the four WT proteins shown in Fig. 6*A*–*D* when in contact with LacdiNAc-presenting GDSs for comparison.

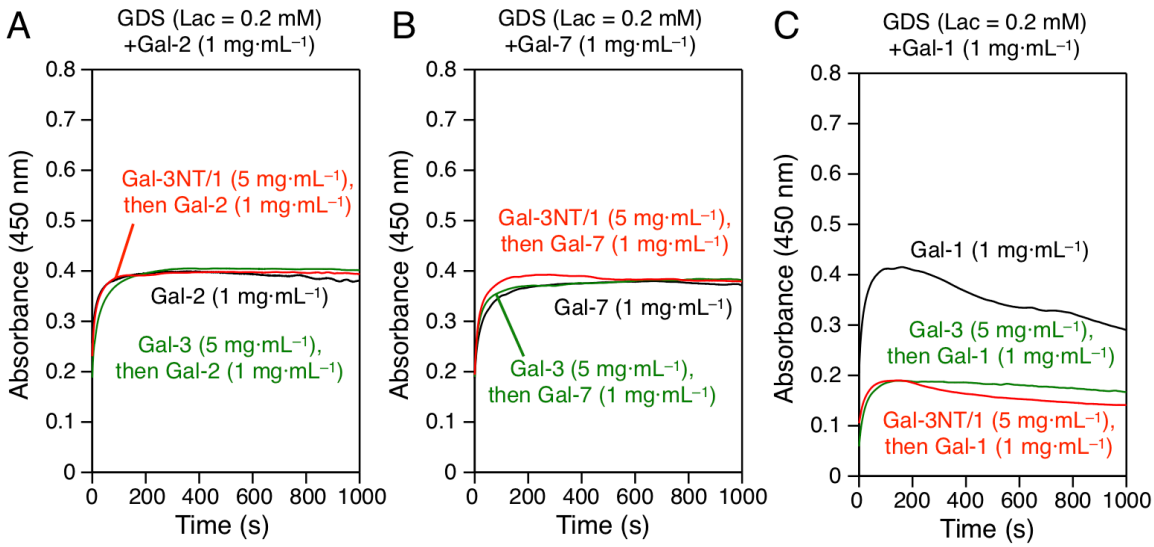

Fig. S26. Aggregation of Lac-presenting GDSs (900 μL, Lac = 0.2 mM) in the competitive mode using chimera-type Gal-3 or Gal-3NT/1 (100 μL, 1 mg/mL) with proto-type Gal-2 (*A*), Gal-7 (*B*) or Gal-1 (*C*) (100 μL, 5 mg/mL).

Table S1: Protein expression conditions and yields. Values are means ± SD.

Proteins	Temperature (°C)	IPTG (µM)	Yield (mg/L)	n
Gal-3NT/1	22	50	8.80 ± 0.97	5
Gal-3—Gal-3	22	100	80.21 ± 24.24	3
Gal-3—8S—Gal-3	22	100	52.58 ± 16.90	4
Gal-3—8L—Gal-3	22	100	48.33 ± 5.77	3
Gal-3—Gal-1	22	100	17.86 ± 9.99	5
Gal-3—8S—Gal-1	22	100	20.72 ± 5.95	7
Gal-1—Gal-3	22	100	81.69 ± 19.45	4
Gal-1—8S—Gal-3	22	100	61.81 ± 18.13	4

Table S2. SAXS data analysis of the galectin variants. Values are means ± SD.

protein	R_g (nm)	D_{max} (nm)	Total	Mw (kDa)	Est. Mw (kDa)
Gal-1–Gal-3	3.64 ± 0.04	11.75 ± 0.25	0.92 ± 0.02	21.32	44.46 ± 1.90
Gal-3–Gal-1	3.12 ± 0.16	9.55 ± 0.76	0.86 ± 0.11	21.32	43.02 ± 0.61
Gal-3–Gal-3*	2.72 ± 0.04	8.18 ± 0.22	0.77 ± 0.12	32.18	32.81 ± 1.30
Gal-1–8S–Gal-1	3.77 ± 0.01	11.60 ± 0.05	0.91 ± 0.05	32.98	31.86 ± 1.78
Gal-1–8S–Gal-3	7.64 ± 0.24	25.00 ± 1.08	0.88 ± 0.03	34.30	68.34 ± 1.81
Gal-3–8S–Gal-1	6.89 ± 0.06	24.50 ± 0.50	0.72 ± 0.01	34.30	70.49 ± 1.22
Gal-3–8S–Gal-3	6.53 ± 0.03	11.35 ± 0.35	0.67 ± 0.07	35.75	34.11 ± 1.85
Gal-3NT/1	4.19 ± 0.38	16.00 ± 0.50	0.72 ± 0.01	24.74	25.18 ± 0.58

*with lactose

Table S3. SAXS data analysis of the galectin chimeras. Values are means ± SD.

	Guinier	GNOM				
	R_g (nm)	R_g (nm)	D_{max} (nm)	Total	Mw	Est. Mw
Gal-1–Gal-3	3.64 ± 0.08	3.64 ± 0.04	11.75 ± 0.25	0.92 ± 0.02	21.32	44.46 ± 1.90
Gal-3–Gal-1	3.16 ± 0.10	3.12 ± 0.16	9.55 ± 0.76	0.86 ± 0.11	21.32	43.02 ± 0.61
Gal-3–Gal-3*	2.68 ± 0.02	2.72 ± 0.04	8.18 ± 0.22	0.77 ± 0.12	32.18	32.81 ± 1.30
Gal-1–8S–Gal-1	3.64 ± 0.15	3.77 ± 0.01	11.60 ± 0.05	0.91 ± 0.05	32.98	31.86 ± 1.78
Gal-1–8S–Gal-3	7.02 ± 0.16	7.64 ± 0.24	25.00 ± 1.08	0.88 ± 0.03	34.30	68.34 ± 1.81
Gal-3–8S–Gal-1	6.80 ± 0.15	6.89 ± 0.06	24.50 ± 0.50	0.72 ± 0.01	34.30	70.49 ± 1.22
Gal-3–8S–Gal-3	3.45 ± 0.11	6.53 ± 0.03	11.35 ± 0.35	0.67 ± 0.07	35.75	34.11 ± 1.85
Gal-3NT/1	3.99 ± 0.16	4.19 ± 0.38	16.00 ± 0.50	0.72 ± 0.01	24.74	25.18 ± 0.58

*in the presence of lactose

Table S4. SAXS model parameters. Values are means ± SD.

Ab intio modelling

	Discrepancy (χ^2)	Nº models	Program (Nº models)	NSD
Gal-1–Gal-3	0.93 ± 0.06	40	Gasbor (20) Dammif (20)	1.54 ± 0.15
Gal-3–Gal-1	1.17 ± 0.27	30	Gasbor (30)	1.34 ± 0.12
Gal-3–Gal-3	1.05 ± 0.06	14	Dammin (14)	1.00 ± 0.05
Gal-1–8S–Gal-1	1.01 ± 0.19	21	Gasbor (10) Dammif (11)	1.25 ± 0.38
Gal-1–8S–Gal-3	1.20 ± 0.19	50	Dammin (50)	0.97 ± 0.20
Gal-3–8S–Gal-1	1.34 ± 0.33	20	Dammin (20)	0.96 ± 0.05
Gal-3–8S–Gal-3	0.87 ± 0.01	20	Dammin (20)	0.88 ± 0.03
Gal-3NT/1	1.38 ± 0.08	20	Dammin (20)	0.77 ± 0.02

Table S5. Data of calorimetric measurements using Lac as ligand. Values are means ± SD.

protein	concentration (μM)	n (sites)	-ΔG (kcal/mol)	-ΔH (kcal/mol)	-TΔS (kcal/mol)	K_d(μM)
Gal-3WT	88.5	0.85	5.38	13.1 ± 0.541	7.73	115 ± 2.99
Gal-3—Gal-3	50	1.66	5.27	11.6 ± 0.316	6.31	137 ± 2.33
Gal-3—8S—Gal-3	33	1.70	5.26	11.6 ± 0.475	6.38	140 ± 9.86

Table S6. Fluorescein/Protein molar ratios (F/P)

Lectin	Protein molar ratio (F/P)*
Gal-1	0.77
Gal-3	0.66
trGal-3	0.66
Gal-3-Gal-3	0.62
Gal-3-8S-Gal-3	0.59
Gal-1-Gal-3	0.67
Gal-3NT/1	0.73

* The F/P molar ratio is defined as the ratio of moles of FITC to moles of protein in the conjugate

References

1 Vértesy S, Michalak M, Miller MC, Schnölzer M, André S, Kopitz J, Mayo KH, Gabius H-J (2015) Structural significance of galectin design: impairment of homodimer stability by linker insertion and partial reversion by ligand presence. *Protein Eng Des Sel* 28:199-210.

2 Zhang S, Moussodia R-O, Murzeau C, Sun HJ, Klein M L, Vértesy S, André S, Roy R, Gabius H-J, Percec V (2015) Dissecting molecular aspects of cell interactions using glycodendrimersomes with programmable glycan presentation and engineered human lectins. *Angew Chem Int Ed* 54:4036-4040.

3 Kopitz J, Xiao Q, Ludwig A-K, Romero A, Michalak M, Sherman SE, Zhou X, Dazen C, Vértesy S, Kaltner H, Klein ML, Gabius H-J, Percec V (2017) Reaction of a programmable glycan presentation of glycodendrimersomes and cells with engineered human lectins to show the sugar functionality of the cell surface. *Angew Chem Int Ed Engl* 56:14677-14681.

4 Pernot P, et al. (2013) Upgraded ESRF BM29 beamline for SAXS on macromolecules in solution. *J Synchrotron Rad* 20*:*660-664.

5 Round A et al. (2015) BioSAXS Sample Changer: a robotic sample changer for rapid and reliable high-throughput X-ray solution scattering*. Acta Cryst D* 71*:*67-75.

6 Svergun DI (1992) Determination of the regularization parameter in indirect-transform methods using perceptual criteria*. J Appl Cryst* 25:495-503.

7 Konarev PV, Volkov VV, Sokolova AV, Koch MHJ, Svergun DI (2003) PRIMUS: a Windows PC-based system for small-angle scattering data analysis. *J Appl Crystallogr* 36:1277-1282.

8 Petoukhov MV et al. (2012) New developments in the ATSAS program package for small-angle scattering data analysis. *J Appl Crystallogr* 45:342-350.

9 Svergun DI, Petoukhov MV, Koch MHJ (2001) Determination of domain structure of proteins from X-ray solution scattering. *Biophys J* 80:2946-2953.

10 Svergun DI (1999) Restoring low resolution structure of biological macromolecules from solution scattering using simulated annealing. *Biophys J* 76:2879-2886.

11 Franke D, Svergun DI (2009) DAMMIF, a program for rapid ab-initio shape determination in small-angle scattering. *J Appl Cryst* 42:342-346.

12 Kozin M, Svergun DI (2001) Automated matching of high- and low-resolution structural models *J Appl Cryst* 34:33-41.

13 Volkov VV, Svergun DI (2003) Uniqueness of ab-initio shape determination in small-angle scattering. *J Appl Cryst* 36:860-864.

14 DeLano, W L (2012) http://www.pymol.org.

15 Wang S, Li W, Liu S & Xu J (2016) RaptorX-Property: a web server for protein structure property prediction. *Nucleic Acids Res* 44:W430-W435.

16 Yang J & Zhang, Y (2015) Protein structure and function prediction using I-TASSER. *Curr Protoc Bioinformatics* 52:5.8.1-5.815.

17 Ruiz FM, Gilles U, Ludwig A-K, Sehad C, Shiao TC, García Caballero G, Kaltner H, Lindner I, Roy R, Reusch D, Romero A, Gabius H-J (2018) Chicken GRIFIN: Structural characterization in crystals and in solution. *Biochimie* 146:127-138.

18 The TH and Feltkamp TEW (1970) Conjugation of fluorescin isothiocyanate to antibodies. I. Experiments on the conditions of conjugation. Immunology 18:865-873.

19 Kopitz J, von Reitzenstein C, Burchert M, Cantz M, Gabius H-J (1998) Galectin-1 is a major receptor for ganglioside GM1, a product of the growth-controlling activity of a cell surface ganglioside sialidase, on human neuroblastoma cells in culture. *J Biol Chem* 273:11205-11211

20 Kato H, Uzawa H, Nagatsuka T, Kondo S, Sato K, Ohsawa I, Kanamori-Kataoka M, Takei Y, Ota S, Furuno M, Dohi H, Nishida Y, Seto Y (2011) Preparation and evaluation of lactose-modified monoliths for the adsorption and decontamination of plant toxins and lectins. *Carbohydr Res* 346:1820-1826.

21 Ellervik U, Magnusson G (1996) Glycosylation with N-Troc-protected glycosyl donors. *Carbohydr Res* 280:251-260.

22 Huang C, Wang N, Fujiki K, Otsuka Y, Akamatsu M, Fujimoto Y, Fukase K (2010) Widely Applicable Deprotection Method of 2,2,2-Trichloroethoxycarbonyl (Troc) Group Using Tetrabutylammonium Fluoride. *J Carbohydr Chem* 29:289–298.

23 Niemietz M, Perkams L, Hoffman J, Eller S, Unverzagt C (2011) Selective oxidative debenzylation of mono- and oligosaccharides in the presence of azides. *Chem Commun* 47:10485–10.

24 Zhang S, et al. (2014) Mimicking biological membranes with programmable glycan ligands self-assembled from amphiphilic Janus glycodendrimers. *Angew Chem Int Ed* 53(41):10899–10903.

25 Zhang S, et al. (2015) Glycodendrimersomes from sequence-defined Janus glycodendrimers reveal high activity and sensor capacity for the agglutination by natural variants of human lectins. *J Am Chem Soc* 137(41):13334–13344.

26 Xiao Q, et al. (2018) Exploring functional pairing between surface glycoconjugates and human galectins using programmable glycodendrimersomes. *Proc Natl Acad Sci USA* 115(11): E2509-E2518.